AFRL-RV-PS-
TR-2017-0156

IMPACT OF POLARIZING NON-LAMBERTIAN SURFACE AND VOLUME SCATTERING ON POLARIZED LIGHT SIGNATURES: IMPORTANCE TO REMOTE SENSING

Knut Stamnes and Zhenyi Lin

Stevens Institute of Technology
1 Castle Point on Hudson
Hoboken, NJ 07030-5906

08 December 2016

Final Report

AIR FORCE RESEARCH LABORATORY
Space Vehicles Directorate
3550 Aberdeen Ave SE
AIR FORCE MATERIEL COMMAND
KIRTLAND AIR FORCE BASE, NM 87117-5776

DTIC COPY

NOTICE AND SIGNATURE PAGE

Using Government drawings, specifications, or other data included in this document for any purpose other than Government procurement does not in any way obligate the U.S. Government. The fact that the Government formulated or supplied the drawings, specifications, or other data does not license the holder or any other person or corporation; or convey any rights or permission to manufacture, use, or sell any patented invention that may relate to them.

This report is the result of contracted fundamental research which is exempt from public affairs security and policy review in accordance with AFI 61-201, paragraph 2.3.5.1. This report is available to the general public, including foreign nationals. Copies may be obtained from the Defense Technical Information Center (DTIC) (http://www.dtic.mil).

AFRL-RV-PS-TR-2017-0156 HAS BEEN REVIEWED AND IS APPROVED FOR PUBLICATION IN ACCORDANCE WITH ASSIGNED DISTRIBUTION STATEMENT.

//SIGNED//	//SIGNED//
Jeannette van den Bosch	Dr. Thomas R. Caudill, Acting Chief
Program Manager, AFRL/RVBYI	AFRL Battlespace Environment Division

This report is published in the interest of scientific and technical information exchange, and its publication does not constitute the Government's approval or disapproval of its ideas or findings.

REPORT DOCUMENTATION PAGE

Form Approved
OMB No. 0704-0188

1. REPORT DATE *(DD-MM-YYYY)*	**2. REPORT TYPE**	**3. DATES COVERED** *(From - To)*
08-12-2016	Final Report	09 Jun 2015 – 01 Oct 2016

4. TITLE AND SUBTITLE
Impact of Polarizing Non-Lambertian Surface and Volume Scattering on Polarized Light Signatures: Importance to Remote Sensing

5a. CONTRACT NUMBER

5b. GRANT NUMBER
FA9453-15-1-0076

5c. PROGRAM ELEMENT NUMBER
62601F

6. AUTHOR(S)
Knut Stamnes and Zhenyi Lin

5d. PROJECT NUMBER
1010

5e. TASK NUMBER
PPM00026607

5f. WORK UNIT NUMBER
EF129628

7. PERFORMING ORGANIZATION NAME(S) AND ADDRESS(ES)
Stevens Institute of Technology
1 Castle Point on Hudson
Hoboken, NJ 07030-5906

8. PERFORMING ORGANIZATION REPORT NUMBER

9. SPONSORING / MONITORING AGENCY NAME(S) AND ADDRESS(ES)
Air Force Research Laboratory
Space Vehicles Directorate
3550 Aberdeen Avenue SE
Kirtland AFB, NM 87117-5776

10. SPONSOR/MONITOR'S ACRONYM(S)
AFRL/RVBYI

11. SPONSOR/MONITOR'S REPORT NUMBER(S)
AFRL-RV-PS-TR-2017-0156

12. DISTRIBUTION / AVAILABILITY STATEMENT

Approved for public release; distribution is unlimited.

13. SUPPLEMENTARY NOTES

14. ABSTRACT
A modernized and upgraded version of the polarized (vector) radiative transfer algorithm VDISORT-OD5 will be used to study the interaction of polarized light with realistic (rough) surfaces. The end goal is to analyze the impact of rough surfaces on polarized light at arbitrary polar angles, and to carry out a sensitivity analysis of the influence of rough surfaces on polarized light. Although thermal radiation is initially unpolarized when emitted in the atmosphere, it becomes polarized by scattering processes with aerosols and clouds and through interactions with polarizing surfaces. The proposed work will analyze the impact of rough surface and volume scattering on polarized light at arbitrary polar angles, and perform a sensitivity analysis of the influence of rough surface and volume scattering on polarized light. Utilization of the polarized bi-directional reflection capabilities in VDISORT-MOD5 will enhance our understanding of the interaction of polarized light with realistic surfaces and is of utmost importance in remote sensing analysis for correct characterization of rough surfaces with respect to fundamental spectral signature development, surface modeling, experimental validation, synthetic image generation, and improvement of both quantitative remote sensing algorithm performance and accuracy assessment of image analysis.

15. SUBJECT TERMS
polarized (vector) radiative transfer, phase matrix, phase function, Stokes parameters, non-Lambertian reflecting surfaces

16. SECURITY CLASSIFICATION OF:			**17. LIMITATION OF ABSTRACT**	**18. NUMBER OF PAGES**	**19a. NAME OF RESPONSIBLE PERSON**
a. REPORT	**b. ABSTRACT**	**c. THIS PAGE**			Jeannette van den Bosch
Unclassified	Unclassified	Unclassified	Unlimited	40	**19b. TELEPHONE NUMBER** *(include area code)*

This page is intentionally left blank.

Table of Contents

List of Figures

Final Performance Report

Award FA9453-15-1-0076

Impact of polarizing non-Lambertian surface and volume scattering on polarized light signatures: Importance to remote sensing

Knut Stamnes, PI
Stevens Institute of Technology

---

1. Summary

In 2015 - 2016, we have focused on upgrading VDISORT to improve the computation of the Stokes components at arbitrary polar viewing angles. We also have carried out sensitivity tests for non-Lambertian surfaces. The work carried out includes the following accomplishments:

- An upgrade of VDISORT to allow for output at arbitrary (user) polar viewing angles for the 3-vector $(I, Q, U)^T$ as well as the 4-vector $(I, Q, U, V)^T$ Stokes vector has been completed. Here ^{T} denotes the transpose.
- An extension from a single layer to a general multiple-layer system has been completed for the user polar viewing angle output.
- The user polar viewing angles output has been extended from working for a black surface only to a partially reflecting surface represented by Lambertian as well as general non-Lambertian surfaces.
- Sensitivity studies of how the user polar angle output depends on the number of streams have been carried out.

2. Upgrade of VDISORT

2.1. General discussion of arbitrary polar user-angle output

The discrete ordinate method provides Stokes vector components at discrete polar angles, called the quadrature angles. However, many practical problems

including remote sensing applications require Stokes vector components at sensor observing angles. Even though one could envision generating results at sensor observing angles by interpolating or extrapolating the quadrature values to such angles, accurate interpolation of these values is difficult, particularly for optical depths close to the top boundary. For example, Fig. 1 shows an example of inaccurate interpolation ('spline') for a benchmark case (Garcia and Siewert, 1989) that has been reproduced by VDISORT. We note that the 'spline' interpo-

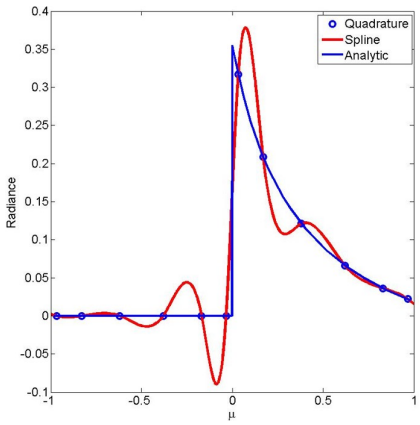

Figure 1: Comparison of output for (i) quadrature angles; (ii) spline interpolation; and (iii) arbitrary angle output ('analytic').

lation produces large oscillations, wheres the integration of the source-function technique, see Eqs. (1) and (2), give accurate ('analytic') results that agree with the benchmark values.

The upgrade of VDISORT to give output at user-specified polar angles, provides a robust and accurate way to generate results at arbitrary polar angles analytically. For a plane parallel atmosphere, the Stokes components at an arbitrary polar angle, $\theta = \cos^{-1}\mu$, can be computed by an integration of the source function. In plane-parallel geometry the Stokes vector $\mathbf{I}(\tau,\mu,\phi) = (I,Q,U,V)^T$, where ^{T} denotes the transpose, can be expanded in a Fourier series in a Fourier series (see Eq. (22) of the Appendix), and the Fourier components can be expressed as

$$\mathbf{I}_\alpha^{m+}(\tau,\mu) = \mathbf{I}_\alpha^{m+}(\tau_b,\mu)e^{-(\tau_b-\tau)/\mu} + \int_\tau^{\tau_b}\frac{dt}{\mu}\mathbf{S}_\alpha^{m+}(t,\mu)e^{-(t-\tau)/\mu} \quad (1)$$

$$\mathbf{I}_\alpha^{m-}(\tau,\mu) = \mathbf{I}_\alpha^{m-}(\tau_0,\mu)e^{-(\tau-\tau_0)/\mu} + \int_{\tau_0}^{\tau}\frac{dt}{\mu}\mathbf{S}_\alpha^{m-}(t,\mu)e^{-(\tau-t)/\mu} \quad (2)$$

at an arbitrary angle $\theta = \cos^{-1}\mu$ in the downward $[\mathbf{I}_\alpha^{m-}(\tau,\mu)]$ and upward $[\mathbf{I}_\alpha^{m+}(\tau,\mu))]$ directions. Here $\tau_0 = 0$ is the optical depth at the top of the slab, and τ_b is the optical thickness of the slab.

A very important reason to develop an analytic arbitrary polar angle output capability in VDISORT is that MODTRAN makes use of this feature, which is

particularly useful when considering spherical refractive geometry. Computation of $\mathbf{I}^{m\pm}(\tau,\mu)$ at arbitrary values of cosine of the polar angle μ based on Eqs. (1) and (2) is similar to that used in the scalar radiative transfer model (DISORT) which has already been implemented into MODTRAN (see MODTRAN ATBD for more details). However, the implementation of VDISORT into MODTRAN becomes more complicated because (i) the four Stokes components are coupled and must be computed together; (ii) the introduction of the 'V' component produces some complex eigenvalues and eigenvectors which require additional attention and processing. To be more specific, we may define the incremental Stokes vector for a line-of-sight (LOS) segment using Eqs. (1) and (2):

$$\Delta\mathbf{I}_\alpha^{m+}(\tau,\mu) = \mathbf{I}_\alpha^{m+}(\tau,\mu) - \mathbf{I}_\alpha^{m+}(\tau_b,\mu)e^{-(\tau_b-\tau)/\mu} = \int_\tau^{\tau_b} \frac{dt}{\mu}\mathbf{S}_\alpha^{m+}(t,\mu)e^{-(t-\tau)/\mu} \tag{3}$$

$$\Delta\mathbf{I}_\alpha^{m-}(\tau,\mu) = \mathbf{I}_\alpha^{m-}(\tau,\mu) - \mathbf{I}_\alpha^{m-}(\tau_0,\mu)e^{-(\tau-\tau_0)/\mu} = \int_{\tau_0}^{\tau} \frac{dt}{\mu}\mathbf{S}_\alpha^{m-}(t,\mu)e^{-(\tau-t)/\mu}. \tag{4}$$

For a single-layer, homogeneous slab, the LOS segment will be a straight line, while for a multi-layer, plane-parallel atmosphere, each layer LOS corresponds to a straight line segment. As explained in some detail in the MODTRAN6 ATBD, in a realistic curved (and refractive) atmosphere, each layer should be divided into several segments, and the value of μ, will be different in each segment along the curved LOS. As in the scalar DISORT case, implementation of arbitrary user-angle output greatly facilitates the computation of LOS segment Stokes components, and the incorporation of VDISORT into MODTRAN in spherical, refractive geometry.

2.2. Analytic representation of the source function

As shown in Section 6.1, the source function can be written as

$$\mathbf{S}_\alpha^m(\tau,u) = \tilde{\mathbf{S}}_\alpha^m(\tau,u) + \mathbf{Q}_\alpha^m(\tau,u) \qquad \alpha = c \text{ or } s \tag{5}$$

where [see Eq. (28)]

$$\mathbf{Q}_\alpha^m(\tau,u) \;=\; \mathbf{X}_\alpha^m(\tau,u)\, e^{-\tau/\mu_0} + \;\delta_{c\alpha}\,\delta_{0m}\,[1-\varpi(\tau)]\,\mathbf{S}_t(\tau) \tag{6}$$

and the contributions due to multiple scattering are given by

$$\begin{aligned}\tilde{\mathbf{S}}_c^m(\tau,u) \;=\; & \frac{\varpi(\tau)}{4}\sum_{\substack{j=-N\\ j\neq 0}}^{N} w_j\Big\{(1+\delta_{0m})\,\mathbf{P}_c^m(\tau,u_j,u)\,\mathbf{I}_c^m(\tau,u_j) \\ & -\mathbf{P}_s^m(\tau,u_j,u)\,\mathbf{I}_s^m(\tau,u_j)\Big\} \;-\; \mathbf{Q}_c^m(\tau,u)\end{aligned} \tag{7}$$

$$\begin{aligned}\tilde{\mathbf{S}}_s^m(\tau,u) \;=\; & \frac{\varpi(\tau)}{4}\sum_{\substack{j=-N\\ j\neq 0}}^{N} w_j\Big\{\mathbf{P}_c^m(\tau,u_j,u)\,\mathbf{I}_s^m(\tau,u_j) \\ & +\mathbf{P}_s^m(\tau,u_j,u)\,\mathbf{I}_c^m(\tau,u_j)\Big\} \;-\; \mathbf{Q}_s^m(\tau,u).\end{aligned} \tag{8}$$

We see that the source function is obtained from a summation of quadrature angle output where μ_j indicates the j^{th} of the $2N$ quadrature angles. For instance, $\mathbf{I}_{\alpha}^{m}(\tau, \mu_j,)$ is the Stokes vector evaluated at the j^{th} quadrature angle μ_j.

2.3. Upgrade of the arbitrary angle output

The upgrade of arbitrary angle output is based on the progress in the previous year. In 2015, the arbitrary angle output could only be computed under a black lower boundary, a single layer and for the first three ($[I, Q, U]^T$) Stokes components. Now in 2016, the arbitrary angle output in VDISORT is improved to provide the support for: (i) the computation of the full Stokes vector output, including the 'V' component; (ii) a multi-layer system; (iii) a reflectance from a general (Non-Lambertian) lower boundary.

2.4. Validation of the arbitrary angle output – black surface

To validate the arbitrary user-angle output, we compared with Kokhanovsky's (Kokhanovsky et al., 2010) benchmark computations of transmittances and reflectances of Stokes vector components for a single medium consisting of either molecules only, aerosols only, or cloud droplets only. The aerosol and cloud particles were considered to be spheres whose Inherent Optical Properties (IOPs) were computed by Mie-theory. In the previous year, we had tested Kokhanovsky's benchmark in the quadrature angles and obtained a good agreement. This year we tested the arbitrary angle output.

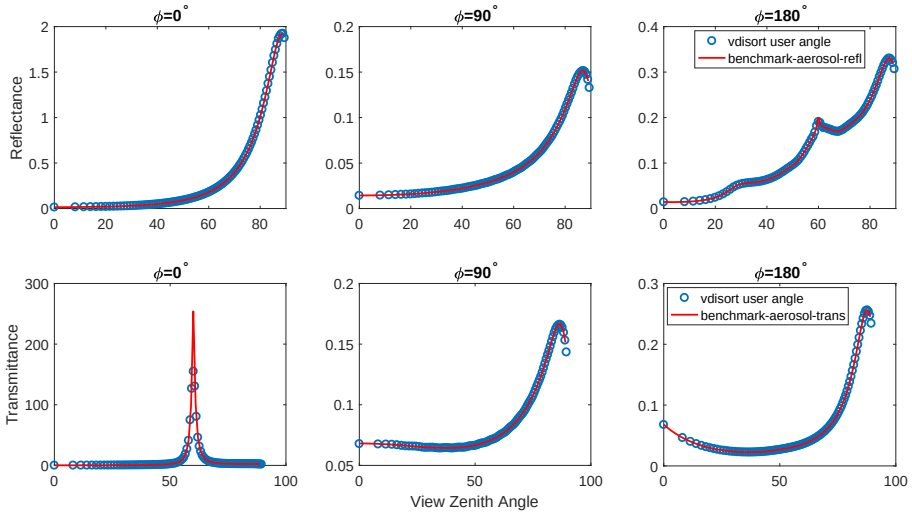

Figure 2: Kokhanovsky's benchmark, I component.

Figures 2–4 show the comparison of benchmark computations for an aerosol case with VDISORT results for 200 polar output angles. In this test we used 192

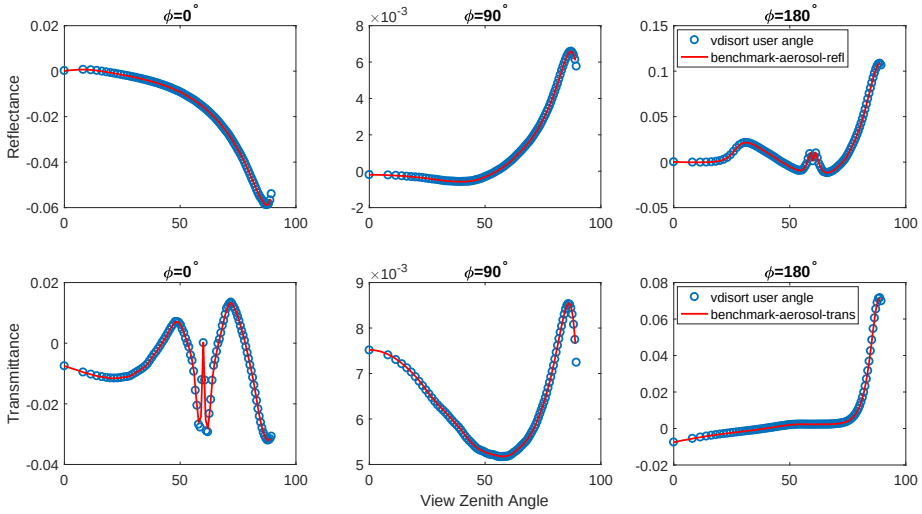

Figure 3: Kokhanovsky's benchmark, Q component.

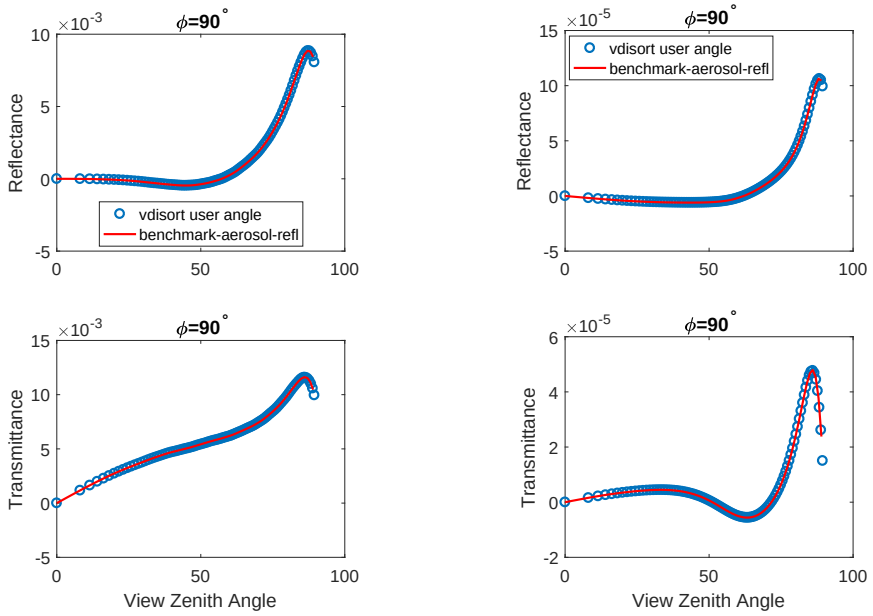

Figure 4: Kokhanovsky's benchmark, U component (left) and V component (right).

streams and Delta-M scaling (Wiscombe, 1977). The 200 user-defined angles are shown as blue circles in each figure with $\cos\theta$ varying from -1.0 to 1.0 in steps of 0.01. In order to test of the user-angle output for a multi-layer system,

we split the single layer into 5 identical layers with the same optical properties and the same total optical thickness as for the single layer. Again, very good agreement was obtained for the user-angle output.

2.5. Validation of user-angle output – wind-roughened ocean surface

A rough ocean surface has also been added to VDISORT and used to test the user-angle output implementation. An explicit expression for the reflectance matrix $\mathbf{R}_{rs}$ at the rough surface interface is given by

$$\begin{aligned}\mathbf{R}_{rs}(\theta_s,\phi_s;\theta_i,\phi_i) &= \frac{1}{\cos\theta_s}\frac{|\mathbf{k}_{1d}|^4}{4|\hat{k}_i\times\hat{k}_s|^4 k_{1dz}^4} \\ &\quad\times\frac{1}{2\pi\sigma^2}\exp\left(-\frac{k_{1dx}^2+k_{1dy}^2}{2k_{1dz}^2\sigma^2}\right)\mathbf{C}_{rs}^r(\theta_s,\phi_s;\theta_i,\phi_i). \quad (9)\end{aligned}$$

The factor

$$p(\alpha,\beta)\equiv\frac{1}{2\pi\sigma^2}\exp\left(-\frac{\alpha^2+\beta^2}{2\sigma^2}\right)\qquad \alpha=\frac{k_{1dx}^2}{k_{1dz}^2},\qquad \beta=\frac{k_{1dy}^2}{k_{1dz}^2}$$

is the probability density of surface slopes resulting from the assumption of a *Gaussian rough surface*, and σ^2 is the mean square *surface slope*.

To test the implementation of the rough surface in VDISORT, we decided to reproduce the SeaDAS Rayleigh tables (Gordon and Wang, 1992). In these tables the TOA radiance contributed from a clear atmosphere (molecular scattering only) overlying a wind-roughened water surface are tabulated. In VDISORT we used a Rayleigh scattering atmospheric layer above a rough surface to reproduce the radiances provided in these SeaDAS tables for a wind speed of 4.21 m/s. We turned off the direct beam reflectance, but kept the diffuse reflectance in order to remove the radiance due to sunglint.

Figures 5–7 show comparisons of radiances at 412 nm for three different azimuth angles, $0°, 90°$, and $180°$, and for a $20°$ solar zenith angle. In general, there is a good match between VDISORT results and the SeaDAS tables with a less than 3% difference. By contrast, a difference up to 10% is found between the result produced by DISORT (green line) and the SeaDAS tables, demonstrating the importance of polarization effects. The full radiance (the blue line), including both the diffuse (skyglint) and the direct beam (sunglint) reflectance, is shown to illustrate how strong the sunglint is at different azimuth angles.

3. Sensitivity Study

The phase matrix for spherical particles is expanded into four independent Greek constants $\alpha_1=\alpha_2$, $\alpha_3=\alpha_4$, β_1, β_2. In Kokhanovsky's benchmark for aerosol particles, each constant is represented by more than 900 terms, which implies that 900 streams would be needed to obtain very accurate results. In the last section, we used 192 streams as well as the Delta-M method (Wiscombe,

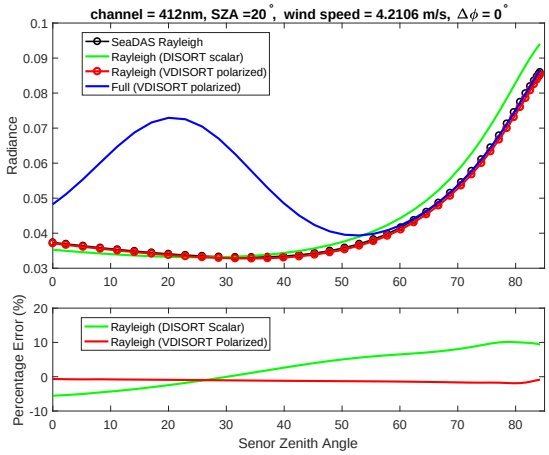

Figure 5: Comparison of SeaDAS Rayleigh tables, VDISORT Rayleigh tables (vector), DISORT Rayleigh tables (scalar), and VDISORT full radiances (vector) for a relative azimuth angle of 0°.

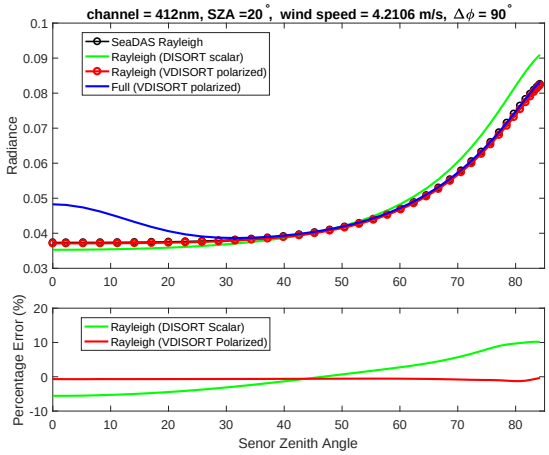

Figure 6: Comparison of SeaDAS Rayleigh tables, VDISORT Rayleigh tables (vector), DISORT Rayleigh tables (scalar), and VDISORT full radiances (vector) for a relative azimuth angle of 90°.

1977) to match the benchmark results and obtained good agreement. However, in practice we generally want to use much fewer streams (e.g. less than 32 streams) because the computational expense increases sharply as the number of streams is increased. To examine how the accuracy depends on the number of streams, we re-computed the aerosol benchmark case using 8, 16, and 32 streams, and compared the results with the accurate 19-stream results. These comparisons are shown in Fig. 8 - 10. We note that the 8- and 16-stream cases (green and blue curves) failed to match the 192-stream results (red curves). The

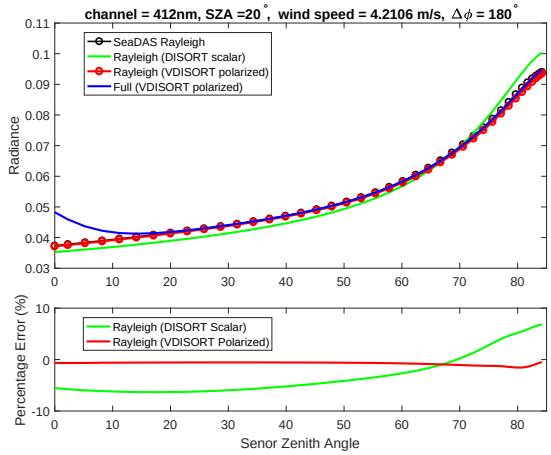

Figure 7: Comparison of SeaDAS Rayleigh tables, VDISORT Rayleigh tables (vector), DISORT Rayleigh tables (scalar), and VDISORT full radiances (vector) for a relative azimuth angle of 180°.

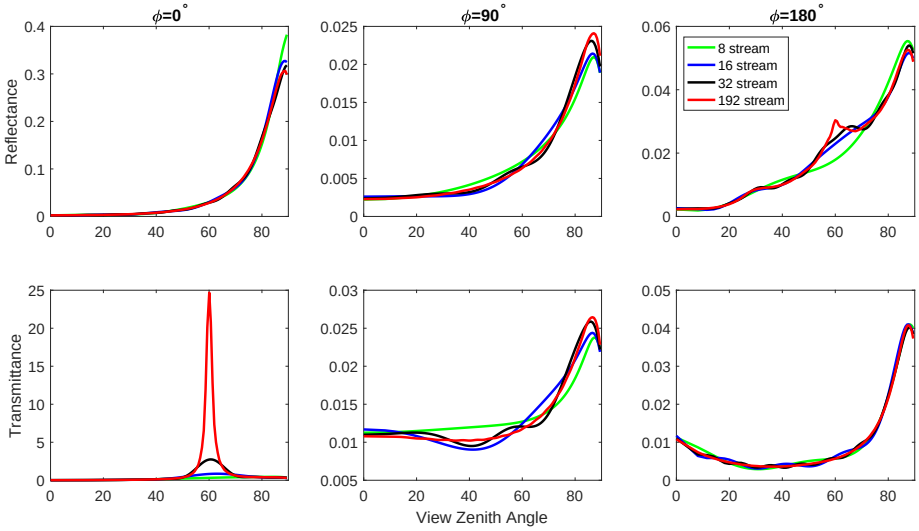

Figure 8: Test of Stream number: I component.

32-stream results (black curves) are close to the 192-stream results, except for the discrepancies around the forward scattering (left bottom subplot, around 60°) and backward scattering angles (right top subplot, around 60°) as well as some oscillations.

To further improve the 32-stream results, we introduced the Delta-Fit method (Hu et al., 2000), which provides a stronger truncation of the forward scattering peak, compared with Delta-M method. Specifically, Delta-Fit method applies

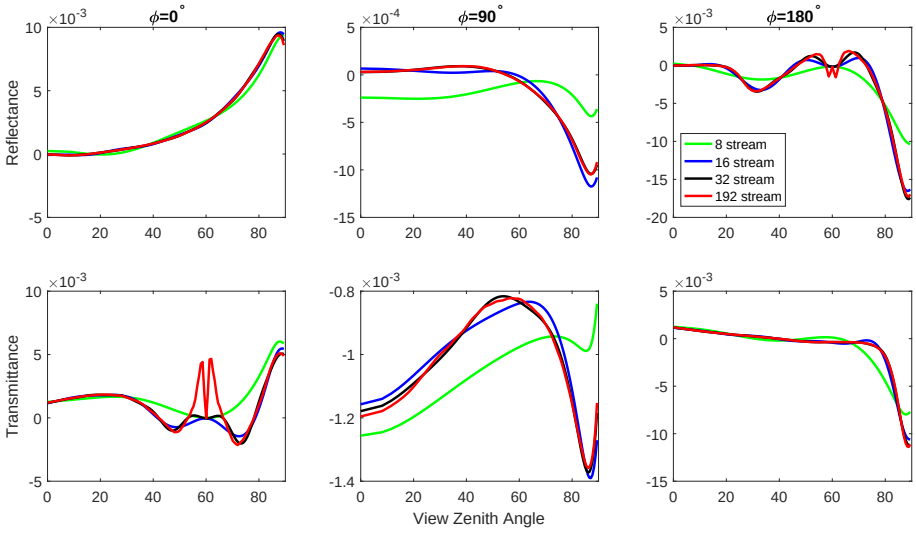

Figure 9: Test of Stream number: Q component.

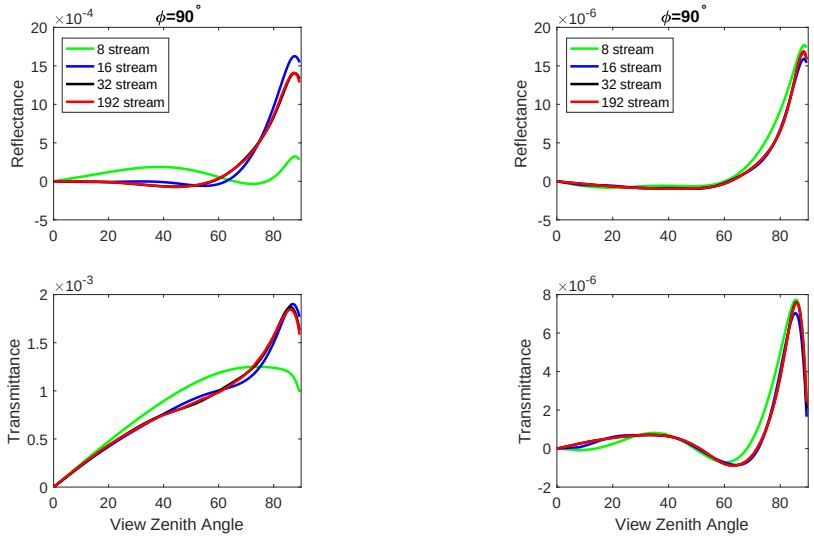

Figure 10: Test of Stream number: U component (left) and V component (right).

a Singular Value Decomposition (SVD) followed by a Least Squares Fitting to the phase matrix to improve the performance for small stream numbers.

To examine the effect of using Delta-Fit, Figures 11 and 12 show the improvement of the I component (radiance) resulting from the use of the Delta-Fit method for 16 and 32 streams. The results of Delta-Fit (red curves) show an

improvement and better match with the 192 stream case (blue curves). The oscillations in 32-stream results without Delta-Fit scaling (green curves) have also been removed.

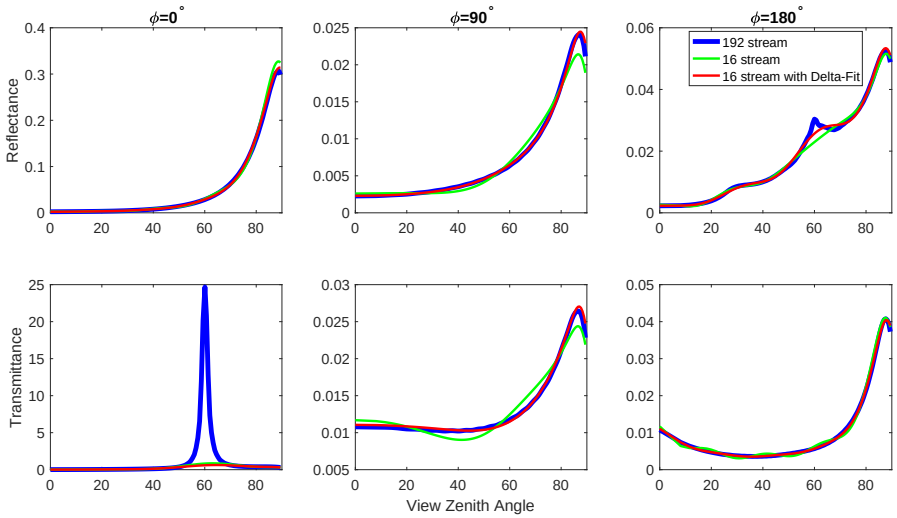

Figure 11: Comparison of I component w/ and w/o DeltaFit for 16 streams.

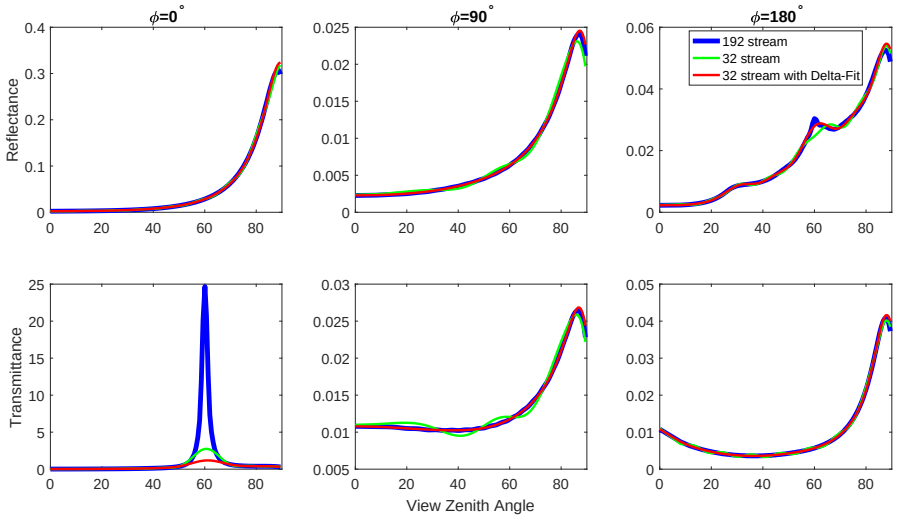

Figure 12: Comparison of I component w/ and w/o DeltaFit for 32 streams.

4. Description of the code

In this section, examples are shown of how to call VDISORT for different conditions.

4.1. Calling VDISORT: benchmark computations and other tests

Table shows a list of benchmark tests for VDISORT. These benchmarks are from Garcia and Siewert (1989), Siewert (2000), and Kokhanovsky et al. (2010).

Script file	Description	Matlab plots
run_kokh2010_rayleigh.sh	Kokhanovsky's Rayleigh benchmark	benchmark_vdisort_kokh_rayleigh.m
run_kokh2010_aerosol.sh	Kokhanovsky's Aerosol benchmark	benchmark_vdisort_kokh_aerosol.m
run_kokh2010_cloud.sh	Kokhanovsky's Cloud benchmark	benchmark_vdisort_kokh_cloud.m
run_siewert1989.sh	Garcia and Siewert (1989) benchmark	benchmark_siewert1989.m
run_siewert2000.sh	Siewert (2000) benchmark	benchmark_siewert2000.m

To run the benchmarks, simply execute the corresponding scripts in the table. To verify that the results are correct, a Matlab code, located in the directory './plots', is provided to produce plots that compare VDISORT output with the benchmark data.

Similarly, there are some other tests for the arbitrary angle output, including multiple (2) layers as well as for a general Non-Lambertian surface shown in table.

Script file	Description
run_usrang_2layers-kokh2010_aerosol.sh	Arbitrary angle and split 2 layers for Kokhanovsky's Aerosol benchmark
run_usrang_2layers_siewert1989.sh	Arbitrary angle and split 2 layers for Garcia and Siewert's benchmark
run_usrang_2layers_siewert2000.sh	Arbitrary angle and split 2 layers for Siewert benchmark in 2000
run_usrang_vacuum_cmbrdf	Arbitrary angle for the Cox-Munk rough surface
run_usrang_rayleigh_cmbrdf	Arbitrary angle for a Rayleigh layer on top of the Cox-Munk rough surface

Finally, there are script tests included in table that can be used to reproduce some DISORT 3 tests. To reproduce the results from the scalar model, all elements of the four by four scattering phase matrix, except the first one, are set to zero.

Script file	Description
run_disort3_case2a.sh	Reproduce DISORT test case 2a: Rayleigh scattering, Beam source
run_disort3_case2b.sh	Reproduce DISORT test case 2b: Rayleigh scattering, Beam source
run_disort3_case2c.sh	Reproduce DISORT test case 2c: Rayleigh scattering, Beam source
run_disort3_case2d.sh	Reproduce DISORT test case 2d: Rayleigh scattering, Beam source
run_disort3_case6c.sh	Reproduce DISORT test case 6c: Lambert surface
run_disort3_case14b.sh	Reproduce DISORT test case 14b: Rough sea surface (Non-Lambertian)

4.2. Model setup

To build the personal settings, one may need to know model setups. Below shows some of important Model inputs:

Name	Description
Lambert	True = lambert surface; False = general surface
ALBEDO	if Lambert = true, it gives the value of albedo
NLYR	number of layers
NLEG	number of GSF terms that expands phase matrix
NAZ	NAZ = NLEG -1
NSTR	NSTR = NLEG
USRANG	True = output in arbitrary angles; False = output in quadrature angles
NUMU	if USRANG = true, it gives the number of arbitrary polar angles
UMU	if USRANG = true, it gives the cosine of arbitrary polar angles (1:NUMU)
USRTAU	True = specify user output optical thickness; False = layer optical thickness
NUTAU	if USRTAU = true, it gives the number of output optical thickness
UTAU	if USRTAU = true, it gives the optical thickness for output (1:NUTAU)
NUPHI	the number of output azimuth angles
UPHI	azimuth angles for output (1:NUPHI)
UMU0	cosine of Solar Zenith Angle
PHI0	solar azimuth angle (PHI0 = 0)
FBEAM	FBEAM = so (solar incidence)

And the following table shows some of important model parameters, which are located in the directory '/src/PARM_F90.h'. It is worth mentioning that once changes have been made to the input constants, it is then necessary to clean all binary files and re-compile the whole model. This "clean-up" can be done by simply going to the "/src" directory and typing the command "gmake clean".

Variable name	Description
Reduce	Reduce='1': apply reduction of order; (fast) Reduce='0': does not apply reduction of order (slow) Recommend to set Reduce='1' to speed up
Complx	Complx='1': compute complex solution $[I,\ Q,\ U,\ V]^T$; Complx='0': ignore V component and compute solution $[I,\ Q,\ U,\ 0]^T$

5. References

Garcia, R., Siewert, C., 1989. The fn method for radiative transfer models that include polarization effects. Journal of Quantitative Spectroscopy and Radiative Transfer 41 (2), 117–145.

Gordon, H. R., Wang, M., 1992. Surface-roughness considerations for atmospheric correction of ocean color sensors. 1: The rayleigh-scattering component. Applied optics 31 (21), 4247–4260.

Hovenier, J. W., van der Mee, C. V. M., 1983. Fundamental relationships relevant to the transfer of polarized light in a scattering atmosphere. Astron. Astrophys. 128, 1–16.

Hu, Y., Wielicki, B., Lin, B., Gibson, G., Tsay, S.-C., Stamnes, K., Wong, T., 2000. δ-fit: A fast and accurate treatment of particle scattering phase functions with weighted singular-value decomposition least-squares fitting. Journal of Quantitative Spectroscopy and Radiative Transfer 65 (4), 681–690.

Kokhanovsky, A. A., Budak, V. P., Cornet, C., Duan, M., Emde, C., Katsev, I. L., Klyukov, D. A., Korkin, S. V., C-Labonnote, L., Mayer, B., et al., 2010. Benchmark results in vector atmospheric radiative transfer. Journal of Quantitative Spectroscopy and Radiative Transfer 111 (12), 1931–1946.

Schulz, F. M., Stamnes, K., Weng, F., 1999. Vdisort: An improved and generalized discrete ordinate radiative transfer model for polarized (vector) radiative transfer computations. J. Quant. Spectrosc. Radiat. Transfer 61, 105–122.

Siewert, C., 2000. A discrete-ordinates solution for radiative-transfer models that include polarization effects. Journal of Quantitative Spectroscopy and Radiative Transfer 64 (3), 227–254.

Stamnes, K., Tsay, S. C., Wiscombe, W. J., Jayaweera, K., 1988. Numerically stable algorithm for discrete-ordinate-method radiative transfer in multiple scattering and emitting layered media. Appl. Opt. 27, 2502–2509.

Stamnes, K., Tsay, S. C., Wiscombe, W. J., Laszlo, I., 2000. DISORT, A General-Purpose Fortran Program for Discrete-Ordinate-Method Radiative Transfer in Scattering and Emitting Layered Media: Documentation of Methodology. NASA report, ftp://climate.gsfc.nasa.gov/pub/wiscombe/Multiple Scatt/.

Strang, G., 2005. Linear algebra and its applications. thomson–brooks. Cole, Belmont, CA, USA.

Weng, F., 1992. A multi-layer discrete-ordinate method for vector radiative transfer in a vertically-inhomogenous, emitting and scattering atmosphere - i. theory. J. Quant. Spectrosc. Radiat. Transfer 47, 19–33.

Wiscombe, W., 1977. The delta-m method: Rapid yet accurate radiative flux calculations for strongly asymmetric phase functions. Journal of the atmospheric sciences 34 (9), 1408–1422.

6. Appendix: Theoretical Background

The radiative transfer equation (RTE) for the total unpolarized radiance, which includes both thermal emission and multiple scattering, can be written

$$\frac{dI_\nu(\tau,\Omega)}{d\tau_s} = -I_\nu(\tau,\Omega) + [1-\varpi(\nu)]B_\nu(T) + \frac{\varpi(\nu)}{4\pi}\int_{4\pi} d\omega' p(\hat{\Omega}',\hat{\Omega}) I_\nu(\tau,\Omega') \quad (10)$$

where $I_\nu(\tau, \Omega)$ is the radiance, $\varpi(\nu)$, the single-scattering albedo, $B_\nu(T)$ the Planck function, and $p(\hat{\Omega}', \hat{\Omega})$ the scattering phase function. For a plane-parallel medium in which the IOPs are assumed to vary only in the vertical direction denoted by z, increasing upwards, so that the corresponding vertical optical depth, denoted by $\tau(z)$, is defined by

$$\tau(z) = \int_z^\infty [\alpha(z') + \beta(z')] dz' \tag{11}$$

and hence

$$d\tau(z) = -[\alpha(\tau) + \beta(\tau)] dz \tag{12}$$

where the minus sign indicates that τ increases in the downward direction, whereas z increases in the upward direction. Equation (10) pertains to the total radiation field. In a plane-parallel geometry, with a collimated beam incident at the top of the slab, one may invoke the usual diffuse-direct splitting to obtain for the diffuse component of the radiation field (omitting the subscript ν and the functional dependence on ν for notational convenience)

$$u \frac{dI(\tau, u, \phi)}{d\tau} = I(\tau, u, \phi) - S(\tau, u, \phi) \tag{13}$$

where

$$\begin{aligned} S(\tau, u, \phi) &= S_b(\tau, u, \phi) + [1 - \varpi(\tau)] B(\tau) \\ &\quad + \frac{\varpi(\tau)}{4\pi} \int_0^{2\pi} d\phi' \int_{-1}^{1} p(\tau, u', \phi'; u, \phi) I(\tau, u', \phi') du. \end{aligned} \tag{14}$$

Here u is the cosine of the polar angle θ, ϕ is the azimuth angle, $\varpi(\tau) = \beta(\tau)/[\alpha(\tau) + \beta(\tau)]$ is the single-scattering albedo, $p(\tau, u', \phi'; u, \phi)$ is the scattering phase function, and $B(\tau)$ is the thermal radiation field given by the Planck function. The term $S_b(\tau, u, \phi)$ in Eq. (14) is the single-scattering source function due to a collimated beam incident at the top of the upper slab, to be specified below.

6.1. RTE for polarized radiation

To generalize Eq. (13) to apply to polarized radiation, we note that the multiple scattering term in Eq. (14) must be replaced by

$$\mathbf{S}(\tau, u, \phi) = \frac{\varpi(\tau)}{4\pi} \int_0^{2\pi} d\phi' \int_{-1}^{1} \mathbf{P}(\tau, u', \phi'; u, \phi) \mathbf{I}(\tau, u', \phi') du \tag{15}$$

where $\mathbf{I}(\tau, u', \phi')$ is the Stokes vector, and $\mathbf{P}(\tau, u', \phi'; u, \phi)$ is the scattering phase matrix. The first element of the vector $\mathbf{S}(\tau, u, \phi)$ represents the energy per unit solid angle, per unit frequency interval, and per unit time that is scattered by a unit volume in the direction (θ, ϕ). Hence, in a plane-parallel (slab) geometry,

the integro-differential equation for polarized radiative transfer is expressed in terms of a Stokes vector $\mathbf{I}(\tau, u, \phi)$ as

$$u\frac{d\,\mathbf{I}(\tau,u,\phi)}{d\tau} \;=\; \mathbf{I}(\tau,u,\phi) - \mathbf{S}(\tau,u,\phi) \tag{16}$$

where the source function is

$$\begin{aligned}\mathbf{S}(\tau,u,\phi) \;&=\; \frac{\varpi(\tau)}{4\pi}\int_0^{2\pi} d\phi' \int_{-1}^{1} du'\,\mathbf{P}(\tau,u',\phi';u,\phi)\mathbf{I}(\tau,u',\phi') \\ &\quad + \mathbf{Q}(\tau,u,\phi).\end{aligned} \tag{17}$$

The term $\mathbf{Q}(\tau, u, \phi)$, due to thermal and beam sources is given by:

$$\mathbf{Q}(\tau,u,\phi) = \frac{\varpi(\tau)}{4\pi}\,\mathbf{P}(\tau,-\mu_0,\phi_0;u,\phi)\mathbf{S}_b e^{-\tau/\mu_0} + \left[1-\varpi(\tau)\right]\mathbf{S}_t(\tau). \tag{18}$$

The first term on the right hand side of Eq. (18) describes the incident beam $\mathbf{S}_b$ in direction $(-\mu_0, \phi_0)$, which is attenuated at depth τ by a factor $e^{-\tau/\mu_0}$ and undergoes single scattering into the direction (u, ϕ). For an unpolarized incident beam $\mathbf{S}_b$ has the form

$$\mathbf{S}_b = [I_0/2, I_0/2, 0, 0]^T \;\text{ or }\; [I_0, 0, 0, 0]^T \tag{19}$$

where the first or second expression corresponds to the choice of Stokes vector representation, $[I_\parallel, I_\perp, U, V]^T$ or $[I, Q, U, V]^T$. The second term on the right hand side of Eq. (18) is due to thermal emission, which is unpolarized and given by

$$\mathbf{S}_t(\tau) = [B(T(\tau))/2, B(T(\tau))/2, 0, 0]^T \;\text{ or }\; [B(T(\tau)), 0, 0, 0]^T \tag{20}$$

where B is the Planck function, and where the first or second expression corresponds to the choice of Stokes vector representation. We have set $\mu_0 \equiv |u_0| \equiv |\cos\theta_0|$, where θ_0 is the polar angle of the incident light beam.

6.1.1. Isolation of azimuth dependence

We start by expanding the phase matrix in a Fourier series:

$$\mathbf{P}(u',u;\phi'-\phi) = \sum_{m=0}^{M}\left\{\mathbf{P}_c^m(u',u)\cos m(\phi'-\phi) + \mathbf{P}_s^m(u',u)\sin m(\phi'-\phi)\right\}. \tag{21}$$

To isolate the azimuth dependence of the radiation field we expand the Stokes vector $\mathbf{I}(\tau, u, \phi)$ in Eq. (16) and the source term $\mathbf{Q}(\tau, u, \phi)$ in Eq. (18) in a Fourier series in a manner similar to the expansion of the phase matrix in Eq. (21):

$$\mathbf{I}(\tau,u,\phi) = \sum_{m=0}^{M}\left\{\mathbf{I}_c^m(\tau,u)\cos m(\phi_0-\phi) + \mathbf{I}_s^m(\tau,u)\sin m(\phi_0-\phi)\right\} \tag{22}$$

$$\mathbf{Q}(\tau,u,\phi) = \sum_{m=0}^{M}\left\{\mathbf{Q}_c^m(\tau,u)\cos m(\phi_0-\phi) + \mathbf{Q}_s^m(\tau,u)\sin m(\phi_0-\phi)\right\} \tag{23}$$

where the subscript s or c denotes sine or cosine mode. Substitution of Eqs. (21) into Eq. (18) and comparison with Eq. (23) yields:

$$\mathbf{Q}_c^m(\tau,u) = \mathbf{X}_c^m(\tau,u)\,e^{-\tau/\mu_0} + \delta_{0m}\,[1-\varpi(\tau)]\,\mathbf{S}_t(\tau) \quad (24)$$

$$\mathbf{Q}_s^m(\tau,u) = \mathbf{X}_s^m(\tau,u)\,e^{-\tau/\mu_0} \quad (25)$$

where

$$\mathbf{X}_c^m(\tau,u) = \frac{\varpi(\tau)}{4\pi}\,\mathbf{P}_c^m(\tau,-\mu_0,u)\,\mathbf{S}_b \quad (26)$$

$$\mathbf{X}_s^m(\tau,u) = \frac{\varpi(\tau)}{4\pi}\,\mathbf{P}_s^m(\tau,-\mu_0,u)\,\mathbf{S}_b \quad (27)$$

which can be written more compactly as (letting $\alpha = c, s$ represent the cosine or sine mode):

$$\mathbf{Q}_\alpha^m(\tau,u) = \mathbf{X}_\alpha^m(\tau,u)\,e^{-\tau/\mu_0} + \delta_{c\alpha}\,\delta_{0m}\,[1-\varpi(\tau)]\,\mathbf{S}_t(\tau) \quad (28)$$

where $\delta_{c\alpha} = 1$ if $\alpha = c$, and $\delta_{c\alpha} = 0$ if $\alpha \neq c$.

By substituting Eqs. (21), (22), and (23) into Eqs. (16) and (17), performing the integration over ϕ' in Eq. (17), and comparing terms of equal order in the resulting Fourier series, one obtains a transfer equation for each Fourier component of the Stokes vector:

$$u\,\frac{d\mathbf{I}_\alpha^m(\tau,u)}{d\tau} = \mathbf{I}_\alpha^m(\tau,u) - \mathbf{S}_\alpha^m(\tau,u) \qquad \alpha = c \text{ or } s, \quad (29)$$

where

$$\mathbf{S}_\alpha^m(\tau,u) = \tilde{\mathbf{S}}_\alpha^m(\tau,u) + \mathbf{Q}_\alpha^m(\tau,u) \quad (30)$$

and the contributions due to multiple scattering are

$$\tilde{\mathbf{S}}_c^m(\tau,u) = \frac{\varpi(\tau)}{4}\int_{-1}^{1} du'\left\{\mathbf{P}_c^m(\tau,u',u)\,\mathbf{I}_c^m(\tau,u')\,(1+\delta_{0m}) - \mathbf{P}_s^m(\tau,u',u)\,\mathbf{I}_s^m(\tau,u')\,(1-\delta_{0m})\right\} \quad (31)$$

$$\tilde{\mathbf{S}}_s^m(\tau,u) = \frac{\varpi(\tau)}{4}\int_{-1}^{1} du'\left\{\mathbf{P}_c^m(\tau,u',u)\,\mathbf{I}_s^m(\tau,u')\,(1+\delta_{0m}) + \mathbf{P}_s^m(\tau,u',u)\,\mathbf{I}_c^m(\tau,u')\,(1-\delta_{0m})\right\}. \quad (32)$$

While the cosine modes start at $m = 0$, the sine modes start at $m = 1$, *i.e.* $\mathbf{I}_s^m(\tau,u)$ and $\mathbf{P}_s^m(\tau,u',u)$ vanish for $m = 0$.

6.2. Solution of the RTE

Half-range quantities in slab geometry

In slab geometry it is convenient to introduce the half-range Stokes vectors ?

$$\mathbf{I}_\alpha^+(\tau,\theta,\phi) \equiv \mathbf{I}_\alpha^+(\tau,\theta\le\pi/2,\phi) = \mathbf{I}_\alpha^+(\tau,\mu,\phi)$$
$$\mathbf{I}_\alpha^-(\tau,\theta,\phi) \equiv \mathbf{I}_\alpha^-(\tau,\theta>\pi/2,\phi) = \mathbf{I}_\alpha^-(\tau,\mu,\phi) \quad (33)$$

where $\alpha = c, s$, and $\mu = |u| = |\cos\theta|$. Note that the sign of μ is given by the superscript of the Stokes vector. For the Fourier components [see Eq. (22)], we have similarly

$$\begin{aligned} \mathbf{I}_\alpha^{m+}(\tau,\theta) &\equiv \mathbf{I}_\alpha^{m+}(\tau,\theta \le \pi/2) = \mathbf{I}_\alpha^{m+}(\tau,\mu) \\ \mathbf{I}_\alpha^{m-}(\tau,\theta) &\equiv \mathbf{I}_\alpha^{m-}(\tau,\theta > \pi/2) = \mathbf{I}_\alpha^{m-}(\tau,\mu). \end{aligned} \tag{34}$$

6.2.1. Formal Solutions

In terms of these half-range quantities, Eq. (29) may written as ($\mu \equiv |u|$)

$$\mu \frac{d\mathbf{I}_\alpha^{m+}(\tau,\mu)}{d\tau} = \mathbf{I}_\alpha^{m+}(\tau,\mu) - \mathbf{S}_\alpha^{m+}(\tau,\mu) \tag{35}$$

$$-\mu \frac{d\mathbf{I}_\alpha^{m-}(\tau,\mu)}{d\tau} = \mathbf{I}_\alpha^{m-}(\tau,\mu) - \mathbf{S}_\alpha^{m-}(\tau,\mu). \tag{36}$$

Using an integrating factor, we readily obtain from Eqs. (35) and (36)

$$\begin{aligned} \frac{d}{d\tau}[\mathbf{I}_\alpha^{m+}(\tau,\mu)e^{-\tau/\mu}] &= \Big[\frac{d\mathbf{I}_\alpha^{m+}(\tau,\mu)}{d\tau} - \frac{1}{\mu}\mathbf{I}_\alpha^{m+}(\tau,\mu)\Big]e^{-\tau/\mu} \\ &= -\frac{\mathbf{S}_\alpha^{m+}(\tau,\mu)}{\mu}e^{-\tau/\mu} \end{aligned} \tag{37}$$

$$\begin{aligned} \frac{d}{d\tau}[\mathbf{I}_\alpha^{m-}(\tau,\mu)e^{\tau/\mu}] &= \Big[\frac{d\mathbf{I}_\alpha^{m-}(\tau,\mu)}{d\tau} + \frac{1}{\mu}\mathbf{I}_\alpha^{m-}(\tau,\mu)\Big]e^{\tau/\mu} \\ &= \frac{\mathbf{S}_{\alpha p}^{m-}(\tau,\mu)}{\mu}e^{\tau/\mu}. \end{aligned} \tag{38}$$

Homogeneous-slab medium

For a homogeneous slab with constant refractive index, we adopt the following notation:

1. τ_0 is the optical depth at the upper boundary (top of the slab);
2. τ_b is the optical depth at the lower boundary (bottom of the slab).

Integrating Eq. (37) from τ_b to τ and Eq. (38) from τ_0 to τ ($\tau_0 \le \tau \le \tau_b$), and solving for $\mathbf{I}_\alpha^{m\pm}(\tau,\mu)$ we obtain

$$\mathbf{I}_\alpha^{m+}(\tau,\mu) = \mathbf{I}_\alpha^{m+}(\tau_b,\mu)e^{-(\tau_b-\tau)/\mu} + \int_\tau^{\tau_b} \frac{dt}{\mu}\mathbf{S}_\alpha^{m+}(t,\mu)e^{-(t-\tau)/\mu} \tag{39}$$

$$\mathbf{I}_\alpha^{m-}(\tau,\mu) = \mathbf{I}_\alpha^{m-}(\tau_0,\mu)e^{-(\tau-\tau_0)/\mu} + \int_{\tau_0}^{\tau} \frac{dt}{\mu}\mathbf{S}_\alpha^{m-}(t,\mu)e^{-(\tau-t)/\mu}. \tag{40}$$

Equations (39) and (40) show that for cases in which the source function $\mathbf{S}_\alpha^{m\pm}(t,\mu)$ is known, one can obtain a solution to the radiative transfer problem by numerical integration.

Inhomogeneous Slab – Multi-Layered Medium

The vertical variation of the IOPs in a slab may be dealt with by dividing it

into a number of adjacent, horizontal layers in which the IOPs are taken to be constant within each layer, but allowed to vary from layer to layer. The number of layers should be large enough to resolve the vertical variation in the IOPs. In such a multi-layered medium, consisting of a total of L layers, we may evaluate the integrals in Eqs. (39) and (40) by integrating layer by layer as follows ($\tau_{\ell-1} \le \tau \le \tau_\ell$ and $\mu > 0$, $\tau_b = \tau_L$, $\tau_0 = 0$):

$$\begin{aligned}\int_\tau^{\tau_L} \frac{dt}{\mu} \mathbf{S}_\alpha^{m+}(t,\mu) e^{-(t-\tau)/\mu} &= \int_\tau^{\tau_\ell} \frac{dt}{\mu} \mathbf{S}_{\alpha,\ell}^{m+}(t,\mu) e^{-(t-\tau)/\mu} \\ &\quad + \sum_{n=\ell+1}^{L} \int_{\tau_{n-1}}^{\tau_n} \frac{dt}{\mu} \mathbf{S}_{\alpha,n}^{m+}(t,\mu) e^{-(t-\tau)/\mu} \quad (41)\end{aligned}$$

$$\begin{aligned}\int_0^{\tau} \frac{dt}{\mu} \mathbf{S}_\alpha^{m-}(t,\mu) e^{-(\tau-t)/\mu} &= \sum_{n=1}^{\ell-1} \int_{\tau_{n-1}}^{\tau_n} \frac{dt}{\mu} \mathbf{S}_{\alpha,n}^{m-}(t,\mu) e^{-(\tau-t)/\mu} \\ &\quad + \int_{\tau_{\ell-1}}^{\tau} \frac{dt}{\mu} \mathbf{S}_{\alpha,\ell}^{m-}(t,\mu)) e^{-(\tau-t)/\mu}. \quad (42)\end{aligned}$$

We can evaluate the integrals in Eqs. (41) and (42) either numerically or analytically if the source function is known. Analytical integration is possible in the case of the discrete ordinate method to be discussed below.

6.2.2. Discrete ordinate method

Equations (29)–(32) can be rewritten as:

$$\begin{aligned}u \frac{d\mathbf{I}_c^m(\tau,u)}{d\tau} &= \mathbf{I}_c^m(\tau,u) - \frac{\varpi(\tau)}{4} \int_{-1}^{1} du' \Big\{ \mathbf{P}_c^m(\tau,u',u)\, \mathbf{I}_c^m(\tau,u')\,(1+\delta_{0m}) \\ &\quad - \mathbf{P}_s^m(\tau,u',u)\, \mathbf{I}_s^m(\tau,u') \Big\} - \mathbf{Q}_c^m(\tau,u) \quad (43) \\ u \frac{d\mathbf{I}_s^m(\tau,u)}{d\tau} &= \mathbf{I}_s^m(\tau,u) - \frac{\varpi(\tau)}{4} \int_{-1}^{1} du' \Big\{ \mathbf{P}_c^m(\tau,u',u)\, \mathbf{I}_s^m(\tau,u') \\ &\quad + \mathbf{P}_s^m(\tau,u',u)\, \mathbf{I}_c^m(\tau,u') \Big\} - \mathbf{Q}_s^m(\tau,u) \quad (44)\end{aligned}$$

where we have omitted the Kronecker-deltas in Eq. (32) and the second Kronecker-delta in Eq. (31) since the cosine modes start at $m = 0$, whereas the sine modes start at $m = 1$, *i.e.* $\mathbf{I}_s^m$ and $\mathbf{P}_s^m$ vanish for $m = 0$. The discrete ordinate method consists of replacing the integration over u' by a discrete sum by introducing the Gaussian quadrature points u_j (the discrete ordinates) and corresponding

weights w_j. One obtains for each Fourier component:

$$u_i \frac{d\mathbf{I}_c^m(\tau,u_i)}{d\tau} = \mathbf{I}_c^m(\tau,u_i) - \frac{\varpi(\tau)}{4} \sum_{\substack{j=-N \\ j\neq 0}}^{N} w_j \Big\{ (1+\delta_{0m})\, \mathbf{P}_c^m(\tau,u_j,u_i)\, \mathbf{I}_c^m(\tau,u_j) - \mathbf{P}_s^m(\tau,u_j,u_i)\, \mathbf{I}_s^m(\tau,u_j) \Big\} - \mathbf{Q}_c^m(\tau,u_i), \qquad i = \pm 1,\ldots,\pm N \tag{45}$$

$$u_i \frac{d\mathbf{I}_s^m(\tau,u_i)}{d\tau} = \mathbf{I}_s^m(\tau,u_i) - \frac{\varpi(\tau)}{4} \sum_{\substack{j=-N \\ j\neq 0}}^{N} w_j \Big\{ \mathbf{P}_c^m(\tau,u_j,u_i)\, \mathbf{I}_s^m(\tau,u_j) + \mathbf{P}_s^m(\tau,u_j,u_i)\, \mathbf{I}_c^m(\tau,u_j) \Big\} - \mathbf{Q}_s^m(\tau,u_i), \qquad i = \pm 1,\ldots,\pm N. \tag{46}$$

The convention for the indices of the quadrature points is such that $u_j < 0$ for $j < 0$, and $u_j > 0$ for $j > 0$. These points are distributed symmetrically about zero, *i.e.* $u_{-j} = -u_j$. The corresponding weights are equal, *i.e.* $w_{-j} = w_j$. In a plane-parallel medium, represented by a horizontal slab, it is convenient to consider the two hemispheres defined by $u < 0$ (downward radiation) and $u > 0$ (upward radiation) separately and to make us of the half-range quantity $\mu \equiv |u|$ introduced previously.

It should be emphasized that the essence of the discrete ordinate method is to convert a pair of coupled integro-differential equations [Eqs. (43) and (44)] into a system of coupled, linear differential equations [Eqs. (45) and (46)] by replacing the integrals with discrete sums. Combining cosine modes of the first two Stokes parameters ($I_\parallel$ and $I_\perp$) with the sine modes of the third and fourth Stokes parameters (U and V) in Eqs. (45) and (46), one obtains a set of coupled differential equations for the half-range $4N$ vectors $\tilde{\mathbf{I}}_c^{m\pm}(\tau,\mu_i) \equiv [I_{\parallel c}^m(\tau,\pm\mu_i), I_{\perp c}^m(\tau,\pm\mu_i), U_s^m(\tau,\pm\mu_i), V_s^m(\tau,\pm\mu_i)]^T$, $i = 1,\ldots,N$, which may be written in matrix form as (Weng, 1992; Schulz et al., 1999)

$$-\mathbf{U}\frac{d\tilde{\mathbf{I}}_c^{m-}}{d\tau} = (\mathbf{1} + \mathbf{A}_{11c}^m)\,\tilde{\mathbf{I}}_c^{m-} + \mathbf{A}_{12c}^m\,\tilde{\mathbf{I}}_c^{m+} - \mathbf{Q}_c^{'m-} \tag{47}$$

$$\mathbf{U}\frac{d\tilde{\mathbf{I}}_c^{m+}}{d\tau} = \mathbf{A}_{21c}^m\,\tilde{\mathbf{I}}_c^{m-} + (\mathbf{1} + \mathbf{A}_{22c}^m)\,\tilde{\mathbf{I}}_c^{m+} - \mathbf{Q}_c^{'m+} \tag{48}$$

where $\mathbf{1}$ denotes the $4N \times 4N$ identity matrix,

$$\mathbf{Q}_c^{'m\pm} = \begin{pmatrix} Q_{\parallel c}^m(\tau,\pm\mu_i) \\ Q_{\perp c}^m(\tau,\pm\mu_i) \\ Q_{Us}^m(\tau,\pm\mu_i) \\ Q_{Vs}^m(\tau,\pm\mu_i) \end{pmatrix}_{4N\times 1} \tag{49}$$

and $\mathbf{U}$ is the $4N \times 4N$ diagonal matrix

$$\mathbf{U} = \begin{pmatrix} \mathbf{U}_\perp & & & \\ & \mathbf{U}_\parallel & & \\ & & \mathbf{U}_U & \\ & & & \mathbf{U}_V \end{pmatrix} \tag{50}$$

where the $N \times N$ diagonal submatrices are given by

$$\mathbf{U}_\perp = \mathbf{U}_\parallel = \mathbf{U}_U = \mathbf{U}_V = \mathrm{diag}(\mu_1, \mu_2, \ldots, \mu_N)^T.$$

The matrices $\mathbf{A}^m_{ijc}$ are defined in Section 6.3.

In a similar manner, by combining sine modes of the first two Stokes parameters ($I_\parallel$ and $I_\perp$) with the cosine modes of the third and fourth Stokes parameters (U and V) in Eqs. (45) and (46), one obtains for the $4N$ vectors $\tilde{\mathbf{I}}^{m\pm}_s(\tau, \mu_i) \equiv [I^m_{\parallel s}(\tau, \pm\mu_i), I^m_{\perp s}(\tau, \pm\mu_i), U^m_c(\tau, \pm\mu_i), V^m_c(\tau, \pm\mu_i)]^T$, $i = 1, \ldots, N$, a set of coupled differential equations, which may be written in matrix form as (Weng, 1992; Schulz et al., 1999)

$$-\mathbf{U}\frac{d\tilde{\mathbf{I}}^{m-}_s}{d\tau} = (\mathbf{1} + \mathbf{A}^m_{11s})\,\tilde{\mathbf{I}}^{m-}_s + \mathbf{A}^m_{12s}\,\tilde{\mathbf{I}}^{m+}_s - \mathbf{Q}^{'m-}_s \tag{51}$$

$$\mathbf{U}\frac{d\tilde{\mathbf{I}}^{m+}_s}{d\tau} = \mathbf{A}^m_{21s}\,\tilde{\mathbf{I}}^{m-}_s + (\mathbf{1} + \mathbf{A}^m_{22s})\,\tilde{\mathbf{I}}^{m+}_s - \mathbf{Q}^{'m+}_s \tag{52}$$

where

$$\mathbf{Q}^{'m\pm}_s = \begin{pmatrix} Q^m_{\parallel s}(\tau, \pm\mu_i) \\ Q^m_{\perp s}(\tau, \pm\mu_i) \\ Q^m_{Uc}(\tau, \pm\mu_i) \\ Q^m_{Vc}(\tau, \pm\mu_i) \end{pmatrix}_{4N\times 1} \tag{53}$$

and the matrices $\mathbf{A}^m_{ijs}$ are defined in Section 6.3.

Equations (47) and (48) or Eqs. (51) and (52) may be re-written as:

$$\frac{d\tilde{\mathbf{I}}^{m-}_\alpha}{d\tau} = \tilde{\mathbf{A}}^m_{11\alpha}\,\tilde{\mathbf{I}}^{m-}_\alpha + \tilde{\mathbf{A}}^m_{12\alpha}\,\tilde{\mathbf{I}}^{m+}_\alpha - \tilde{\mathbf{Q}}^{m-}_\alpha \qquad \alpha = c, s \tag{54}$$

$$\frac{d\tilde{\mathbf{I}}^{m+}_\alpha}{d\tau} = \tilde{\mathbf{A}}^m_{21\alpha}\,\tilde{\mathbf{I}}^{m-}_\alpha + \tilde{\mathbf{A}}^m_{22\alpha}\,\tilde{\mathbf{I}}^{m+}_\alpha - \tilde{\mathbf{Q}}^{m+}_\alpha \qquad \alpha = c, s \tag{55}$$

or as

$$\frac{d}{d\tau}\begin{bmatrix} \tilde{\mathbf{I}}^{m-}_\alpha \\ \tilde{\mathbf{I}}^{m+}_\alpha \end{bmatrix} = \begin{pmatrix} \tilde{\mathbf{A}}^m_{11\alpha} & \tilde{\mathbf{A}}^m_{12\alpha} \\ \tilde{\mathbf{A}}^m_{21\alpha} & \tilde{\mathbf{A}}^m_{22\alpha} \end{pmatrix}\begin{bmatrix} \tilde{\mathbf{I}}^{m-}_\alpha \\ \tilde{\mathbf{I}}^{m+}_\alpha \end{bmatrix} - \begin{bmatrix} \tilde{\mathbf{Q}}^{m-}_\alpha \\ \tilde{\mathbf{Q}}^{m+}_\alpha \end{bmatrix} \qquad \alpha = c, s \tag{56}$$

where $\tilde{\mathbf{A}}^m_{11\alpha} = -\mathbf{U}^{-1}(\mathbf{1} + \mathbf{A}^m_{11\alpha})$, $\tilde{\mathbf{A}}^m_{12\alpha} = -\mathbf{U}^{-1}\mathbf{A}^m_{12\alpha}$, $\tilde{\mathbf{A}}^m_{21\alpha} = \mathbf{U}^{-1}\mathbf{A}^m_{21\alpha}$, $\tilde{\mathbf{A}}^m_{22\alpha} = \mathbf{U}^{-1}(\mathbf{1} + \mathbf{A}^m_{22\alpha})$, and $\tilde{\mathbf{Q}}^{m\pm}_\alpha = \mathbf{U}^{-1}\mathbf{Q}^{'m\pm}_\alpha$.

Combining the vectors for the downward and upward directions by defining the $8N$ vectors $\tilde{\mathbf{I}}^m_\alpha \equiv [\tilde{\mathbf{I}}^{m-}_\alpha(\mu_i), \tilde{\mathbf{I}}^{m+}_\alpha(\mu_i)]^T$, and $\tilde{\mathbf{Q}}^m_\alpha \equiv [\tilde{\mathbf{Q}}^{m-}_\alpha(\mu_i), \tilde{\mathbf{Q}}^{m+}_\alpha(\mu_i)]^T$

$(i = 1, \ldots, N)$ we may write the coupled system of differential equations in the following compact form (Weng, 1992; Schulz et al., 1999):

$$\frac{d\tilde{\mathbf{I}}_\alpha^m}{d\tau} = \tilde{\mathbf{A}}_\alpha^m \tilde{\mathbf{I}}_\alpha^m - \tilde{\mathbf{Q}}_\alpha^m \qquad \alpha = c, s \tag{57}$$

where the matrix $\tilde{\mathbf{A}}_\alpha^m$ is given by

$$\tilde{\mathbf{A}}_\alpha^m \equiv \begin{pmatrix} \tilde{\mathbf{A}}_{11\alpha}^m & \tilde{\mathbf{A}}_{12\alpha}^m \\ \tilde{\mathbf{A}}_{21\alpha}^m & \tilde{\mathbf{A}}_{22\alpha}^m \end{pmatrix} \qquad \alpha = c, s. \tag{58}$$

The slab is divided into a number of adjacent layers, large enough to resolve vertical changes in the IOPs. Equation (57) applies in each layer of the slab. As described in some detail in Section 6.3, the solution involves the following steps:

1. the homogeneous version of (57) with $\tilde{\mathbf{Q}}_\alpha^m = 0$ yields a linear combination of exponential solutions (with unknown coefficients) obtained by solving an algebraic eigenvalue problem;
2. analytic particular solutions are found by solving a system of linear algebraic equations;
3. the general solution is obtained by adding the homogeneous and particular solutions;
4. the solution is completed by imposing boundary conditions at the top and the bottom of the slab;
5. the solutions are required to satisfy continuity conditions across layer interfaces in the slab;
6. the application of boundary and layer interface conditions leads to a system of linear algebraic equations, and the numerical solution of this system of equations yields the unknown coefficients in the homogenous solutions.

6.3. Discrete ordinate equations – Compact matrix formulation

As shown in Section 6.2.2 each Fourier component of the RTE satisfies the following equations $(i = \pm 1, \ldots, \pm N)$:

$$\begin{aligned} u_i \frac{d\mathbf{I}_c^m(\tau, u_i)}{d\tau} &= \mathbf{I}_c^m(\tau, u_i) - \frac{\varpi(\tau)}{4} \sum_{\substack{j=-N \\ j\neq 0}}^{N} w_j \Big\{ (1+\delta_{0m})\, \mathbf{P}_c^m(\tau, u_j, u_i)\, \mathbf{I}_c^m(\tau, u_j) \\ &\quad - \mathbf{P}_s^m(\tau, u_j, u_i)\, \mathbf{I}_s^m(\tau, u_j) \Big\} - \mathbf{Q}_c^m(\tau, u_i) \end{aligned} \tag{59}$$

$$\begin{aligned} u_i \frac{d\mathbf{I}_s^m(\tau, u_i)}{d\tau} &= \mathbf{I}_s^m(\tau, u_i) - \frac{\varpi(\tau)}{4} \sum_{\substack{j=-N \\ j\neq 0}}^{N} w_j \Big\{ \mathbf{P}_c^m(\tau, u_j, u_i)\, \mathbf{I}_s^m(\tau, u_j) \\ &\quad + \mathbf{P}_s^m(\tau, u_j, u_i)\, \mathbf{I}_c^m(\tau, u_j) \Big\} - \mathbf{Q}_s^m(\tau, u_i). \end{aligned} \tag{60}$$

As a consequence of certain symmetry relations, the Fourier components of the phase matrix have the following form (Hovenier and van der Mee, 1983):

$$\mathbf{P}_c^m = \begin{pmatrix} P_{11c}^m & P_{12c}^m & 0 & 0 \\ P_{21c}^m & P_{22c}^m & 0 & 0 \\ 0 & 0 & P_{33c}^m & P_{34c}^m \\ 0 & 0 & P_{43c}^m & P_{44c}^m \end{pmatrix} \equiv \begin{pmatrix} \mathbf{P}_{1c}^m & \mathbf{0} \\ \mathbf{0} & \mathbf{P}_{2c}^m \end{pmatrix} \tag{61}$$

$$\mathbf{P}_s^m = \begin{pmatrix} 0 & 0 & P_{13s}^m & P_{14s}^m \\ 0 & 0 & P_{23s}^m & P_{24s}^m \\ P_{31s}^m & P_{32s}^m & 0 & 0 \\ P_{41s}^m & P_{42s}^m & 0 & 0 \end{pmatrix} \equiv \begin{pmatrix} \mathbf{0} & \mathbf{P}_{1s}^m \\ \mathbf{P}_{2s}^m & \mathbf{0} \end{pmatrix} \tag{62}$$

where we have introduced (2×2) block matrices for notational convenience.

6.3.1. "Cosine" solutions

As discussed in Section 6.2.2, by combining cosine modes of the first two Stokes parameters ($I_\parallel$ and $I_\perp$) with the sine modes of the third and fourth Stokes parameters (U and V) in Eqs. (59) and (60), one obtains a set of coupled differential equations for the half-range $4N$ vectors $\tilde{\mathbf{I}}_c^{m\pm}(\tau, \mu_i)$, which may be written in matrix form as

$$\frac{d\tilde{\mathbf{I}}_c^{m-}}{d\tau} = \tilde{\mathbf{A}}_{11c}^m \tilde{\mathbf{I}}_c^{m-} + \tilde{\mathbf{A}}_{12c}^m \tilde{\mathbf{I}}_c^{m+} - \tilde{\mathbf{Q}}_c^{m-} \tag{63}$$

$$\frac{d\tilde{\mathbf{I}}_c^{m+}}{d\tau} = \tilde{\mathbf{A}}_{21c}^m \tilde{\mathbf{I}}_c^{m-} + \tilde{\mathbf{A}}_{22c}^m \tilde{\mathbf{I}}_c^{m+} - \tilde{\mathbf{Q}}_c^{m+} \tag{64}$$

where $\tilde{\mathbf{A}}_{11c}^m = -\mathbf{U}^{-1}(\mathbf{1} + \mathbf{A}_{11c}^m)$, $\tilde{\mathbf{A}}_{12c}^m = -\mathbf{U}^{-1}\mathbf{A}_{12c}^m$, $\tilde{\mathbf{A}}_{21c}^m = \mathbf{U}^{-1}\mathbf{A}_{21c}^m$, $\tilde{\mathbf{A}}_{22c}^m = \mathbf{U}^{-1}(\mathbf{1} + \mathbf{A}_{22c}^m)$, and $\tilde{\mathbf{Q}}_c^{m\pm} = \mathbf{U}^{-1}\mathbf{Q}_c^{m\pm}$. Here $\mathbf{U}$ is a $4N \times 4N$ diagonal block matrix [see Eq. (50)] given by

$$\mathbf{U} = \text{diag}(\mathbf{U}_\perp,\ \mathbf{U}_\parallel,\ \mathbf{U}_U,\ \mathbf{U}_V)^T \tag{65}$$

where the $N \times N$ diagonal submatrices are given by

$$\mathbf{U}_N \equiv \mathbf{U}_\perp = \mathbf{U}_\parallel = \mathbf{U}_U = \mathbf{U}_V = \text{diag}(\mu_1, \mu_2, \ldots, \mu_N)^T \tag{66}$$

and

$$\tilde{\mathbf{I}}_c^{m\pm} = \begin{pmatrix} I_{\parallel c}^m(\tau, \pm\mu_i) \\ I_{\perp c}^m(\tau, \pm\mu_i) \\ U_s^m(\tau, \pm\mu_i) \\ V_s^m(\tau, \pm\mu_i) \end{pmatrix}_{4N\times 1} \qquad \mathbf{S}_c^{m\pm} = \begin{pmatrix} Q_{\parallel c}^m(\tau, \pm\mu_i) \\ Q_{\perp c}^m(\tau, \pm\mu_i) \\ Q_{Us}^m(\tau, \pm\mu_i) \\ Q_{Vs}^m(\tau, \pm\mu_i) \end{pmatrix}_{4N\times 1} \tag{67}$$

and the $4N \times 4N$ matrices $\mathbf{A}_{11c}^m$, $\mathbf{A}_{12c}^m$, $\mathbf{A}_{21c}^m$ and $\mathbf{A}_{22c}^m$ are identical expressions evaluated at different pairs of angles:

$$\mathbf{A}_{11c}^m(\tau) \equiv -w_j \frac{\varpi(\tau)}{4} \begin{pmatrix} (1+\delta_{0m})\mathbf{P}_{1c}^m & -\mathbf{P}_{1s}^m \\ \mathbf{P}_{2s}^m & \mathbf{P}_{2c}^m \end{pmatrix} \Bigg|_{-\mu_i, -\mu_j;\ i,j=1,\ldots,N} \tag{68}$$

$$\mathbf{A}^m_{12c}(\tau) \equiv -w_j \frac{\varpi(\tau)}{4} \left(\begin{array}{cc} (1+\delta_{0m})\mathbf{P}^m_{1c} & -\mathbf{P}^m_{1s} \\ \mathbf{P}^m_{2s} & \mathbf{P}^m_{2c} \end{array} \right) \Bigg|_{-\mu_i, +\mu_j;\ i,j=1,\ldots,N} \tag{69}$$

$$\mathbf{A}^m_{21c}(\tau) \equiv -w_j \frac{\varpi(\tau)}{4} \left(\begin{array}{cc} (1+\delta_{0m})\mathbf{P}^m_{1c} & -\mathbf{P}^m_{1s} \\ \mathbf{P}^m_{2s} & \mathbf{P}^m_{2c} \end{array} \right) \Bigg|_{+\mu_i, -\mu_j;\ i,j=1,\ldots,N} \tag{70}$$

$$\mathbf{A}^m_{22c}(\tau) \equiv -w_j \frac{\varpi(\tau)}{4} \left(\begin{array}{cc} (1+\delta_{0m})\mathbf{P}^m_{1c} & -\mathbf{P}^m_{1s} \\ \mathbf{P}^m_{2s} & \mathbf{P}^m_{2c} \end{array} \right) \Bigg|_{+\mu_i, +\mu_j;\ i,j=1,\ldots,N} \tag{71}$$

where we have used $w_{-j} = w_j$.

We also showed in Section 6.2.2 that we may combine the vectors for the downward and upward directions in Eqs. (63) and (64) by defining the $8N$ vectors, $i = 1, \ldots, N$, $\tilde{\mathbf{I}}^m_c \equiv [\tilde{\mathbf{I}}^{m-}_c(\mu_i), \tilde{\mathbf{I}}^{m+}_c(\mu_i)]^T$, and $\tilde{\mathbf{Q}}^m_c \equiv [\tilde{\mathbf{Q}}^{m-}_c(\mu_i), \tilde{\mathbf{Q}}^{m+}_c(\mu_i)]^T$, so that we may write the coupled system of differential equations for these "cosine" solutions as

$$\frac{d\tilde{\mathbf{I}}^m_c}{d\tau} = \tilde{\mathbf{A}}^m_c \tilde{\mathbf{I}}^m_c - \tilde{\mathbf{Q}}^m_c \tag{72}$$

where the matrix $\tilde{\mathbf{A}}^m_c$ is given by

$$\tilde{\mathbf{A}}^m_c \equiv \left(\begin{array}{cc} \tilde{\mathbf{A}}^m_{11c} & \tilde{\mathbf{A}}^m_{12c} \\ \tilde{\mathbf{A}}^m_{21c} & \tilde{\mathbf{A}}^m_{22c} \end{array} \right)_{8N \times 8N} . \tag{73}$$

We arrived at Eq. (72) by combining cosine modes of the first two Stokes parameters ($I_\parallel$ and $I_\perp$) with the sine modes of the third and fourth Stokes parameters (U and V) in Eqs. (59) and (60), and then by combining the resulting Eqs. (63) and (64) for the upper and lower hemispheres into a single equation for the $8N$ Stokes vector.

Remark: if the incident beam has no U, V components, as for the disk-integrated solar pseudo-source, then the homogeneous "cosine" solutions obtained by solving Eq. (72) completely describe the homogeneous solutions because the "sine" solutions described below vanish.

6.3.2. "Sine" solutions

In a similar manner, by combining the sine modes of the first two Stokes parameters ($I_\parallel$ and $I_\perp$) with the cosine modes of the third and fourth Stokes parameters (U and V) in Eqs. (59) and (60), one obtains for the $4N$ vectors $\tilde{\mathbf{I}}^{m\pm}_s \equiv [I^m_{\parallel s}(\tau, \pm\mu_i), I^m_{\perp s}(\tau, \pm\mu_i), U^m_c(\tau, \pm\mu_i), V^m_c(\tau, \pm\mu_i)]^T$, a set of coupled differential equations given by [see Eqs. (51) and (52) and Eqs. (54) and (55)]

$$\frac{d\tilde{\mathbf{I}}^{m-}_s}{d\tau} = \tilde{\mathbf{A}}^m_{11s}\, \tilde{\mathbf{I}}^{m-}_s + \tilde{\mathbf{A}}^m_{12s}\, \tilde{\mathbf{I}}^{m+}_s - \tilde{\mathbf{Q}}^{m-}_s \tag{74}$$

$$\frac{d\tilde{\mathbf{I}}^{m+}_s}{d\tau} = \tilde{\mathbf{A}}^m_{21s}\, \tilde{\mathbf{I}}^{m-}_s + \mathbf{A}^m_{22s}\, \tilde{\mathbf{I}}^{m+}_s - \tilde{\mathbf{Q}}^{m+}_s \tag{75}$$

where $\tilde{\mathbf{A}}^m_{11s} = -\mathbf{U}^{-1}(\mathbf{1} + \mathbf{A}^m_{11s})$, $\tilde{\mathbf{A}}^m_{12s} = -\mathbf{U}^{-1}\mathbf{A}^m_{12s}$, $\tilde{\mathbf{A}}^m_{21s} = \mathbf{U}^{-1}\mathbf{A}^m_{21s}$, $\tilde{\mathbf{A}}^m_{22s} = \mathbf{U}^{-1}(\mathbf{1}+\mathbf{A}^m_{22s})$, and $\tilde{\mathbf{Q}}^{m\pm}_s = \mathbf{U}^{-1}\mathbf{Q}^{'m\pm}_s$. The matrix $\mathbf{U}$ is the $4N \times 4N$ diagonal matrix given by Eq. (65) and

$$\tilde{\mathbf{I}}^{m\pm}_s = \begin{pmatrix} I^m_{\|s}(\tau, \pm\mu_i) \\ I^m_{\perp s}(\tau, \pm\mu_i) \\ U^m_c(\tau, \pm\mu_i) \\ V^m_c(\tau, \pm\mu_i) \end{pmatrix}_{4N\times 1} \qquad \mathbf{Q}^{'m\pm}_s = \begin{pmatrix} Q^m_{\|s}(\tau, \pm\mu_i) \\ Q^m_{\perp s}(\tau, \pm\mu_i) \\ Q^m_{Uc}(\tau, \pm\mu_i) \\ Q^m_{Vc}(\tau, \pm\mu_i) \end{pmatrix}_{4N\times 1} . \tag{76}$$

The $4N \times 4N$ matrices $\mathbf{A}^m_{11s}$, $\mathbf{A}^m_{12s}$, $\mathbf{A}^m_{21s}$, and $\mathbf{A}^m_{22s}$ are identical expressions evaluated at different pairs of angles:

$$\mathbf{A}^m_{11s}(\tau) \equiv -w_j \frac{\varpi(\tau)}{4} \begin{pmatrix} \mathbf{P}^m_{1c} & \mathbf{P}^m_{1s} \\ -\mathbf{P}^m_{2s} & (1+\delta_{0m})\mathbf{P}^m_{2c} \end{pmatrix} \Bigg|_{-\mu_i, -\mu_j;\, i,j=1,\ldots,N} \tag{77}$$

$$\mathbf{A}^m_{12s}(\tau) \equiv -w_j \frac{\varpi(\tau)}{4} \begin{pmatrix} \mathbf{P}^m_{1c} & \mathbf{P}^m_{1s} \\ -\mathbf{P}^m_{2s} & (1+\delta_{0m})\mathbf{P}^m_{2c} \end{pmatrix} \Bigg|_{-\mu_i, +\mu_j;\, i,j=1,\ldots,N} \tag{78}$$

$$\mathbf{A}^m_{21s}(\tau) \equiv -w_j \frac{\varpi(\tau)}{4} \begin{pmatrix} \mathbf{P}^m_{1c} & \mathbf{P}^m_{1s} \\ -\mathbf{P}^m_{2s} & (1+\delta_{0m})\mathbf{P}^m_{2c} \end{pmatrix} \Bigg|_{+\mu_i, -\mu_j;\, i,j=1,\ldots,N} \tag{79}$$

$$\mathbf{A}^m_{22s}(\tau) \equiv -w_j \frac{\varpi(\tau)}{4} \begin{pmatrix} \mathbf{P}^m_{1c} & \mathbf{P}^m_{1s} \\ -\mathbf{P}^m_{2s} & (1+\delta_{0m})\mathbf{P}^m_{2c} \end{pmatrix} \Bigg|_{+\mu_i, +\mu_j;\, i,j=1,\ldots,N} . \tag{80}$$

Combining Eqs. (74) and (75), we obtain the following equation for the $8N$ Stokes vector

$$\frac{d\tilde{\mathbf{I}}^m_s}{d\tau} = \tilde{\mathbf{A}}^m_s \tilde{\mathbf{I}}^m_s - \tilde{\mathbf{Q}}^m_s \tag{81}$$

which is of a form identical to Eq. (72). Here

$$\tilde{\mathbf{A}}^m_s \equiv \begin{pmatrix} \tilde{\mathbf{A}}^m_{11s} & \tilde{\mathbf{A}}^m_{12s} \\ \tilde{\mathbf{A}}^m_{21s} & \tilde{\mathbf{A}}^m_{22s} \end{pmatrix}_{8N\times 8N} ; \quad \tilde{\mathbf{I}}^m_s \equiv \begin{pmatrix} \tilde{\mathbf{I}}^{m-}_s \\ \tilde{\mathbf{I}}^{m+}_s \end{pmatrix}_{8N\times 1} ; \quad \tilde{\mathbf{Q}}^m_s \equiv \begin{pmatrix} \tilde{\mathbf{Q}}^{m-}_s \\ \tilde{\mathbf{Q}}^{m+}_s \end{pmatrix}_{8N\times 1} .$$

The "sine" solutions found by solving Eq. (81) are necessary for beam sources with non-zero U, V components.

6.4. Discrete ordinate solutions

The vector radiative transfer equations [Eqs. (72) and (81)] have the same form for "cosine" and "sine" combinations. Thus, we may rewrite Eqs. (72) and (81) as

$$\frac{d\tilde{\mathbf{I}}^m_\alpha(\tau)}{d\tau} = \tilde{\mathbf{A}}^m_\alpha(\tau)\tilde{\mathbf{I}}^m_\alpha(\tau) - \tilde{\mathbf{Q}}^m_\alpha(\tau) \qquad \alpha = c, s. \tag{82}$$

6.4.1. Homogeneous solution

For a homogeneous slab with a constant single-scattering albedo $\varpi(\tau) = \varpi$ and phase matrix $\mathbf{P}(\tau, u', u) = \mathbf{P}(u', u)$, the matrix $\tilde{\mathbf{A}}^m_\alpha(\tau)$ will also be independent of position τ in the slab. Therefore, we may seek solutions of the homogeneous version of Eq. (82) [setting $\tilde{\mathbf{Q}}^m_\alpha(\tau) = 0$] of the following form

$$\tilde{\mathbf{I}}^m_\alpha(\tau) = \mathbf{G}^m_\alpha e^{-\lambda^m \tau}. \tag{83}$$

Substituting this expression into Eq. (82) with $\tilde{\mathbf{Q}}^m_\alpha(\tau) = 0$, we find

$$\tilde{\mathbf{A}}^m_\alpha \mathbf{G}^m_\alpha = -\lambda^m \mathbf{G}^m_\alpha. \tag{84}$$

Solving this algebraic eigenvalue problem, we get $8N$ eigenvalues $\lambda^m_{\alpha 1}, ..., \lambda^m_{\alpha 8N}$ with corresponding eigenvectors $\mathbf{G}^m_{\alpha 1}, ..., \mathbf{G}^m_{\alpha 8N}$. The general solution to the homogeneous version of Eq. (82) is a linear combination of these $8N$ linearly independent solutions of the form given by Eq. (83).

We may start with Eqs. (63) and (64) for the cosine modes and Eqs. (74) and (75) for the sine modes and rewrite the homogenous version of these equations as

$$\frac{d\tilde{\mathbf{I}}^{m-}_\alpha}{d\tau} = \tilde{\mathbf{A}}^m_{11\alpha}\, \tilde{\mathbf{I}}^{m-}_\alpha + \tilde{\mathbf{A}}^m_{12\alpha}\, \tilde{\mathbf{I}}^{m+}_\alpha \qquad \alpha = c, s \tag{85}$$

$$\frac{d\tilde{\mathbf{I}}^{m+}_\alpha}{d\tau} = \tilde{\mathbf{A}}^m_{21\alpha}\, \tilde{\mathbf{I}}^{m-}_\alpha + \tilde{\mathbf{A}}^m_{22\alpha}\, \tilde{\mathbf{I}}^{m+}_\alpha \qquad \alpha = c, s. \tag{86}$$

Dropping the superscript m and the subscript α, and seeking solutions to Eqs. (85) and (86) of the form

$$\tilde{\mathbf{I}}^{\pm}(\tau, \pm\mu_i) = \mathbf{G}^{\pm} e^{-k\tau} \qquad \mathbf{G}^{\pm} = \mathbf{G}(k, \pm\mu_i) \tag{87}$$

one finds upon invoking the symmetry relations $\tilde{\mathbf{A}}_{21} = -\tilde{\mathbf{A}}_{12}$ and $\tilde{\mathbf{A}}_{22} = -\tilde{\mathbf{A}}_{11}$ implied by the symmetry of the phase matrix ($i = 1, \ldots, N$):

$$-k\mathbf{G}^- = \tilde{\mathbf{A}}_{11}\, \mathbf{G}^- + \tilde{\mathbf{A}}_{12}\, \mathbf{G}^+ \tag{88}$$

$$-k\mathbf{G}^+ = -\tilde{\mathbf{A}}_{12}\, \mathbf{G}^- - \tilde{\mathbf{A}}_{11}\, \mathbf{G}^+. \tag{89}$$

Addition and subtraction of Eqs. (88) and (89) yields

$$-k(\mathbf{G}^- + \mathbf{G}^+) = (\tilde{\mathbf{A}}_{11} - \tilde{\mathbf{A}}_{12})(\mathbf{G}^- - \mathbf{G}^+) \tag{90}$$

$$-k(\mathbf{G}^- - \mathbf{G}^+) = (\tilde{\mathbf{A}}_{11} + \tilde{\mathbf{A}}_{12})(\mathbf{G}^- + \mathbf{G}^+) \tag{91}$$

which in combination gives

$$(\tilde{\mathbf{A}}_{11} - \tilde{\mathbf{A}}_{12})(\tilde{\mathbf{A}}_{11} + \tilde{\mathbf{A}}_{12})(\mathbf{G}^- + \mathbf{G}^+) = k^2(\mathbf{G}^- + \mathbf{G}^+) \tag{92}$$

$$(\tilde{\mathbf{A}}_{11} + \tilde{\mathbf{A}}_{12})(\tilde{\mathbf{A}}_{11} - \tilde{\mathbf{A}}_{12})(\mathbf{G}^- - \mathbf{G}^+) = k^2(\mathbf{G}^- - \mathbf{G}^+). \tag{93}$$

Solving the eigenvalue problem given by Eq. (92), one obtains eigenvalues k^2 and corresponding eigenvectors

$$\mathbf{G}^+ + \mathbf{G}^- \equiv \mathbf{\Gamma} \tag{94}$$

so that Eq. (91) yields

$$\mathbf{G}^+ - \mathbf{G}^- = \frac{1}{k}(\tilde{\mathbf{A}}_{11} + \tilde{\mathbf{A}}_{12})\mathbf{\Gamma}. \tag{95}$$

Combining Eqs. (94) and (95), one finds

$$\mathbf{G}^+ = \frac{1}{2}\Big[\mathbf{\Gamma} + \frac{1}{k}(\tilde{\mathbf{A}}_{11} + \tilde{\mathbf{A}}_{12})\mathbf{\Gamma}\Big] \tag{96}$$

$$\mathbf{G}^- = \frac{1}{2}\Big[\mathbf{\Gamma} - \frac{1}{k}(\tilde{\mathbf{A}}_{11} + \tilde{\mathbf{A}}_{12})\mathbf{\Gamma}\Big] \tag{97}$$

which on noting that

$$\mathbf{G}^+_{-j} = \mathbf{G}^+(-k_j) = \mathbf{G}^-(k_j) = \mathbf{G}^-_j, \qquad j = 1, 2, \ldots, 4N \tag{98}$$

so that $\mathbf{G}^{\pm}(+k_j) = \mathbf{G}^{\mp}(-k_j)$ provides all the information needed for the solution of Eqs. (85) and (86).

There are a total of $4N$ eigenvalues $\lambda_i = k_i^2, i = 1, \ldots, 4N$ and hence a total of $8N$ eigenvalues occurring in positive/negative pairs:

$$k_j = \sqrt{\lambda_j} > 0, \quad j = 1, \ldots, 4N \tag{99}$$

$$k_{-j} = -k_j, \quad j = 1, \ldots, 4N. \tag{100}$$

Since both real and complex eigensolutions may be present, the complex-variable eigensolver DGEEV of LAPACK [http://www.netlib.org/lapack/lapack-3.5.0.html] may be used to get the solutions. If the eigensolutions are known to be real (as for Rayleigh scattering), the faster routine ASYMTX available in DISORT (Stamnes et al., 1988, 2000) may be used.

The solution to Eqs. (85) and (86) can be written as ($i = 1, \ldots, N$)

$$\mathbf{I}^+_h(\tau) = \mathbf{I}_h(\tau, +\mu_i) = \sum_{\substack{j=-4N \\ j\neq 0}}^{4N} C_j \mathbf{G}^+_j e^{-k_j\tau} = \sum_{j=1}^{4N}[C_j \mathbf{G}^+_j e^{-k_j\tau} + C_{-j}\mathbf{G}^-_j e^{+k_j\tau}] \tag{101}$$

and

$$\mathbf{I}^-_h(\tau) = \mathbf{I}_h(\tau, -\mu_i) = \sum_{\substack{j=-4N \\ j\neq 0}}^{4N} C_j \mathbf{G}^-_j e^{-k_j\tau} = \sum_{j=1}^{4N}[C_j \mathbf{G}^-_j e^{-k_j\tau} + C_{-j}\mathbf{G}^+_j e^{+k_j\tau}] \tag{102}$$

or more compactly as

$$\mathbf{I}^{\pm}_h(\tau) = \mathbf{I}_h(\tau, \pm\mu_i) = \sum_{j=1}^{4N}[C_j \mathbf{G}^{\pm}_j e^{-k_j\tau} + C_{-j}\mathbf{G}^{\mp}_j e^{+k_j\tau}] \tag{103}$$

where $\{C_j\}$ and $\{C_{-j}\}$ are constants of integration to be determined by the boundary conditions.

Since both the eigenvalues $\{k_j\}$ and the eigenvectors $\mathbf{G}^{\pm}(k_j) = \mathbf{G}^{\mp}(-k_j)$ may be complex, it is desirable to rewrite Eqs. (101) and (102) in terms of real quantities. To that end, one may distinguish between real and complex eigenvalues $\{k_j\}$. The eigenvalues (and the associated eigenvectors) of a real matrix are either real or they occur in complex conjugate pairs (Strang, 2005). Thus, letting J_r denote the number of real eigenvalues and J_x denote the number of complex conjugate pairs of eigenvalues, one may write Eqs. (101) and (102) as

$$\mathbf{I}_h^{\pm}(\tau) = \mathbf{I}_{r,h}^{\pm}(\tau) + \Re\{\mathbf{I}_{x,h}^{\pm}(\tau)\} \tag{104}$$

where the real-valued solutions are

$$\mathbf{I}_{r,h}^{+}(\tau) = \sum_{j=1}^{J_r}[C_j\mathbf{G}_j^{+}e^{-k_j\tau} + C_{-j}\mathbf{G}_j^{-}e^{+k_j\tau}] \tag{105}$$

$$\mathbf{I}_{r,h}^{-}(\tau) = \sum_{j=1}^{J_r}[C_j\mathbf{G}_j^{-}e^{-k_j\tau} + C_{-j}\mathbf{G}_j^{+}e^{+k_j\tau}] \tag{106}$$

and the complex-valued solutions are

$$\mathbf{I}_{x,h}^{+}(\tau) = \sum_{j=1}^{J_x}[C_{x,j}\mathbf{G}_{x,j}^{+}e^{-k_{x,j}\tau} + C_{x,-j}\mathbf{G}_{x,j}^{-}e^{+k_{x,j}\tau}] \tag{107}$$

$$\mathbf{I}_{x,h}^{-}(\tau) = \sum_{j=1}^{J_x}[C_{x,j}\mathbf{G}_{x,j}^{-}e^{-k_{x,j}\tau} + C_{x,-j}\mathbf{G}_{x,j}^{+}e^{+k_{x,j}\tau}] \tag{108}$$

where the subscript x (last letter in the word complex) is used to indicate that a quantity is a complex number or eigenvector. Taking the real parts of Eqs. (107) and (108), we find ($C_{x,j} = C_{R,j} + iC_{I,j}$)

$$\begin{aligned}\Re\{\mathbf{I}_{x,h}^{+}(\tau)\} \;=\; & \sum_{j=1}^{J_x}\Big\{C_{R,j}\mathbf{F}_R^{+}(\tau,k_j) + C_{R,-j}\mathbf{F}_R^{-}(\tau,-k_j) \\ & - C_{I,j}\mathbf{F}_I^{+}(\tau,k_j) - C_{I,-j}\mathbf{F}_I^{-}(\tau,-k_j)\Big\}\end{aligned} \tag{109}$$

$$\begin{aligned}\Re\{\mathbf{I}_{x,h}^{-}(\tau)\} \;=\; & \sum_{j=1}^{J_x}\Big\{C_{R,j}\mathbf{F}_R^{-}(\tau,k_j) + C_{R,-j}\mathbf{F}_R^{+}(\tau,-k_j) \\ & - C_{I,j}\mathbf{F}_I^{-}(\tau,k_j) - C_{I,-j}\mathbf{F}_I^{+}(\tau,-k_j)\Big\}\end{aligned} \tag{110}$$

where

$$\mathbf{F}_R^{\pm}(\tau,\pm k_j) \equiv \big[\Re\{\mathbf{G}_{x,j}^{\pm}\}\Re\{e^{\mp k_{x,j}\tau}\} - \Im\{\mathbf{G}_{x,j}^{\pm}\}\Im\{e^{\mp k_{x,j}\tau}\}\big] \tag{111}$$

$$\mathbf{F}_I^{\pm}(\tau,\pm k_j) \equiv \big[\Re\{\mathbf{G}_{x,j}^{\pm}\}\Im\{e^{\mp k_{x,j}\tau}\} + \Im\{\mathbf{G}_{x,j}^{\pm}\}\Re\{e^{\mp k_{x,j}\tau}\}\big]. \tag{112}$$

Note that all the $8N = 2(J_r + 2J_x)$ constants ($2J_r$ values of $C_{\pm j}$, and $2J_x$ values each of $C_{R,\pm j}$ and $C_{I,\pm j}$) in Eqs. (105)–(112) are to be determined by applying the boundary conditions.

6.4.2. Vertically inhomogeneous medium

For a vertically inhomogeneous medium, one may divide the slab into L adjacent homogeneous layers labeled by the index $\ell = 1, \ldots, L$. The IOPs (the phase matrix and the single-scattering albedo) are assumed to be constant within each layer, but they are allowed to vary from layer to layer as required to adequately resolve their vertical variation. Then, the solution arrived at above [Eq. (83)] will be applicable to each layer separately. The exposition may be simplified by rewriting the homogeneous solution given by Eq. (103) for mode $\alpha = c$ or s and layer denoted by ℓ as

$$\mathbf{I}^{m\pm,h}_{\alpha\ell}(\tau) = \sum_{j=1}^{4N} [C^m_{-\alpha j\ell} \mathbf{G}^{m\pm}_{-\alpha j\ell} e^{+k^m_{\alpha j\ell}\tau} + C^m_{\alpha j\ell} \mathbf{G}^{m\pm}_{\alpha j\ell} e^{-k^m_{\alpha j\ell}\tau}]. \tag{113}$$

Defining $\tilde{\mathbf{I}}^m_{\alpha\ell}(\tau) \equiv [\mathbf{I}^{m-}_{\alpha\ell}(\tau), \mathbf{I}^{m+}_{\alpha\ell}(\tau)]^T$, $\tilde{C}_{\alpha j\ell} \equiv [C_{-\alpha j\ell}, C_{\alpha j\ell}]^T$, $\tilde{\mathbf{G}}_{\alpha j\ell} \equiv [\mathbf{G}_{-\alpha j\ell}, \mathbf{G}_{\alpha j\ell}]^T$, one may write Eq. (113) representing the solution to the homogeneous part of the RTE for a Fourier mode denoted by the subscript α and a component denoted by the superscript m in a layer denoted by subscript ℓ more compactly as

$$\tilde{\mathbf{I}}^{m,h}_{\alpha\ell}(\tau) = \sum_{j=1}^{8N} \tilde{C}^m_{\alpha j\ell} \tilde{\mathbf{G}}^m_{\alpha j\ell} e^{-k^m_{\alpha j\ell}\tau} \qquad \ell = 1, \ldots, L. \tag{114}$$

6.4.3. Particular solution

The source term $\tilde{\mathbf{Q}}^m_\alpha(\tau)$ in Eq. (82) for the cosine modes is given by

$$\tilde{\mathbf{Q}}^m_c \equiv \begin{pmatrix} \tilde{\mathbf{Q}}^{m-}_c \\ \tilde{\mathbf{Q}}^{m+}_c \end{pmatrix}_{8N\times 1} \qquad ; \qquad \tilde{\mathbf{Q}}^{m\pm}_c = \begin{pmatrix} \tilde{Q}^m_{\|c}(\tau, \pm\mu_i) \\ \tilde{Q}^m_{\perp c}(\tau, \pm\mu_i) \\ \tilde{Q}^m_{Us}(\tau, \pm\mu_i) \\ \tilde{Q}^m_{Vs}(\tau, \pm\mu_i) \end{pmatrix}_{4N\times 1}$$

and for the sine modes

$$\tilde{\mathbf{Q}}^m_s \equiv \begin{pmatrix} \tilde{\mathbf{Q}}^{m-}_s \\ \tilde{\mathbf{Q}}^{m+}_s \end{pmatrix}_{8N\times 1} \qquad ; \qquad \tilde{\mathbf{Q}}^{m\pm}_s = \begin{pmatrix} \tilde{Q}^m_{\|s}(\tau, \pm\mu_i) \\ \tilde{Q}^m_{\perp s}(\tau, \pm\mu_i) \\ \tilde{Q}^m_{Uc}(\tau, \pm\mu_i) \\ \tilde{Q}^m_{Vc}(\tau, \pm\mu_i) \end{pmatrix}_{4N\times 1}$$

where ($\alpha = c, s$) $\tilde{\mathbf{Q}}^{m\pm}_\alpha(\tau, \mu_i) = \mathbf{U}^{-1}\mathbf{Q}^{'m\pm}_\alpha(\tau, \mu_i)$ and

$$\mathbf{Q}^{'m\pm}_\alpha(\tau, \mu_i) = \mathbf{X}^{m\pm}_\alpha(\tau, \mu_i)\, e^{-\tau/\mu_0} + \delta_{c\alpha}\, \mathbf{B}_{0m}(\tau). \tag{115}$$

Here $\mathbf{X}^{m\pm}_\alpha(\tau, \mu_i) = \frac{\varpi(\tau)}{4\pi}\, \mathbf{P}^m_\alpha(\tau, -\mu_0, \pm\mu_i)\, \mathbf{S}_b$. Thus, the source term $\tilde{\mathbf{Q}}^m_\alpha(\tau, \mu_i)$ in Eq. (82) can be written for each layer denoted by subscript ℓ:

$$\tilde{\mathbf{Q}}^m_{\alpha\ell}(\mu_i) = [\tilde{\mathbf{X}}^m_{\alpha\ell}(\mu_i)\, e^{-\tau/\mu_0} + \delta_{c\alpha}\, \tilde{\mathbf{B}}_{0m,\ell}] \tag{116}$$

where $\tilde{\mathbf{X}}^m_{\alpha\ell}(\mu_i) = \mathbf{U}^{-1}[\mathbf{X}^{m-}_{\alpha\ell}(\mu_i), \mathbf{X}^{m+}_{\alpha\ell}(\mu_i)]^T$, and $\tilde{\mathbf{B}}_{0m,\ell} = \delta_{0m}\,[1-\varpi_\ell]\,\mathbf{U}^{-1}\mathbf{S}_{t\ell}$ [see Eq. (28)].

Cosine modes

Combining the two upper rows of the matrix $\mathbf{P}^m_c$ and the two lower rows of the matrix $\mathbf{P}^m_s$ given by [see Eqs. (61) and (62)]

$$\mathbf{P}^m_c = \begin{pmatrix} P^m_{11c} & P^m_{12c} & 0 & 0 \\ P^m_{21c} & P^m_{22c} & 0 & 0 \\ 0 & 0 & P^m_{33c} & P^m_{34c} \\ 0 & 0 & P^m_{43c} & P^m_{44c} \end{pmatrix} \;\; ; \;\; \mathbf{P}^m_s = \begin{pmatrix} 0 & 0 & P^m_{13s} & P^m_{14s} \\ 0 & 0 & P^m_{23s} & P^m_{24s} \\ P^m_{31s} & P^m_{32s} & 0 & 0 \\ P^m_{41s} & P^m_{42s} & 0 & 0 \end{pmatrix}$$

one obtains a matrix $\tilde{\mathbf{P}}^m_c$ and a corresponding vector $\tilde{\mathbf{S}}_b$ defined as

$$\tilde{\mathbf{P}}^m_c = \begin{pmatrix} P^m_{11c} & P^m_{12c} & 0 & 0 \\ P^m_{21c} & P^m_{22c} & 0 & 0 \\ P^m_{31s} & P^m_{32s} & 0 & 0 \\ P^m_{41s} & P^m_{42s} & 0 & 0 \end{pmatrix}_{8N_1\times 8N_1} \qquad ; \qquad \tilde{\mathbf{S}}_b = \begin{pmatrix} S_{\parallel b} \\ S_{\perp b} \\ S_{Ub} \\ S_{Vb} \end{pmatrix}_{8N_1\times 1} . \tag{117}$$

Hence, for the cosine modes we obtain

$$\begin{aligned} \tilde{\mathbf{X}}^m_c &= \frac{\varpi(\tau)}{4\pi} \begin{pmatrix} P^m_{11c} & P^m_{12c} & 0 & 0 \\ P^m_{21c} & P^m_{22c} & 0 & 0 \\ P^m_{31s} & P^m_{32s} & 0 & 0 \\ P^m_{41s} & P^m_{42s} & 0 & 0 \end{pmatrix}_{8N_1\times 8N_1} \begin{pmatrix} S_{\parallel b} \\ S_{\perp b} \\ S_{Ub} \\ S_{Vb} \end{pmatrix}_{8N_1\times 1} \\ &= \frac{\varpi(\tau)}{4\pi}\tilde{\mathbf{P}}^m_c\tilde{\mathbf{S}}_b = \frac{\varpi(\tau)}{4\pi}\tilde{\mathbf{P}}^m_{c,b} \end{aligned} \tag{118}$$

where the vector $\tilde{\mathbf{P}}^m_{c,b} \equiv \tilde{\mathbf{P}}^m_c\tilde{\mathbf{S}}_b$ is given by

$$\tilde{\mathbf{P}}^m_{b,c} = \begin{pmatrix} P^m_{11c}(\tau,-\mu_0,-\mu^a_i)S_{\parallel b} + P^m_{12c}(\tau,-\mu_0,-\mu^a_i)S_{\perp b} \\ P^m_{21c}(\tau,-\mu_0,-\mu^a_i)S_{\parallel b} + P^m_{22c}(\tau,-\mu_0,-\mu^a_i)S_{\perp b} \\ P^m_{31s}(\tau,-\mu_0,-\mu^a_i)S_{\parallel b} + P^m_{32s}(\tau,-\mu_0,-\mu^a_i)S_{\perp b} \\ P^m_{41s}(\tau,-\mu_0,-\mu^a_i)S_{\parallel b} + P^m_{42s}(\tau,-\mu_0,-\mu^a_i)S_{\perp b} \\ P^m_{11c}(\tau,-\mu_0,+\mu^a_i)S_{\parallel b} + P^m_{12c}(\tau,-\mu_0,+\mu^a_i)S_{\perp b} \\ P^m_{21c}(\tau,-\mu_0,+\mu^a_i)S_{\parallel b} + P^m_{22c}(\tau,-\mu_0,+\mu^a_i)S_{\perp b} \\ P^m_{31s}(\tau,-\mu_0,+\mu^a_i)S_{\parallel b} + P^m_{32s}(\tau,-\mu_0,+\mu^a_i)S_{\perp b} \\ P^m_{41s}(\tau,-\mu_0,+\mu^a_i)S_{\parallel b} + P^m_{42s}(\tau,-\mu_0,+\mu^a_i)S_{\perp b} \end{pmatrix}_{8N_1\times 1} .$$

Sine modes

For the sine modes one may proceed in a similar manner by combining the two upper rows of the matrix $\mathbf{P}^m_s$ and the two lower rows of the matrix $\mathbf{P}^m_c$ to obtain

$$\tilde{\mathbf{P}}^m_s = \begin{pmatrix} 0 & 0 & P^m_{13s} & P^m_{14s} \\ 0 & 0 & P^m_{23s} & P^m_{24s} \\ 0 & 0 & P^m_{33c} & P^m_{34c} \\ 0 & 0 & P^m_{43c} & P^m_{44c} \end{pmatrix}_{8N_1\times 8N_1} \tag{119}$$

Hence, for the sine modes, one obtains

$$\tilde{\mathbf{X}}_s^m = \frac{\varpi(\tau)}{4\pi}\tilde{\mathbf{P}}_s^m\,\tilde{\mathbf{S}}_b = \frac{\varpi(\tau)}{4\pi}\tilde{\mathbf{P}}_{s,b}^m \tag{120}$$

where the vector $\tilde{\mathbf{P}}_{s,b}^m = \tilde{\mathbf{P}}_s^m\,\tilde{\mathbf{S}}_b$ is given by

$$\tilde{\mathbf{P}}_{s,b}^m = \begin{pmatrix} P_{13s}^m(\tau,-\mu_0,-\mu_i^a)S_{Ub} + P_{14s}^m(\tau,-\mu_0,-\mu_i^a)S_{Vb} \\ P_{23s}^m(\tau,-\mu_0,-\mu_i^a)S_{Ub} + P_{24s}^m(\tau,-\mu_0,-\mu_i^a)S_{Vb} \\ P_{33c}^m(\tau,-\mu_0,-\mu_i^a)S_{Ub} + P_{34c}^m(\tau,-\mu_0,-\mu_i^a)S_{Vb} \\ P_{43c}^m(\tau,-\mu_0,-\mu_i^a)S_{Ub} + P_{44c}^m(\tau,-\mu_0,-\mu_i^a)S_{Vb} \\ P_{13s}^m(\tau,-\mu_0,+\mu_i^a)S_{Ub} + P_{14s}^m(\tau,-\mu_0,+\mu_i^a)S_{Vb} \\ P_{23s}^m(\tau,-\mu_0,+\mu_i^a)S_{Ub} + P_{24s}^m(\tau,-\mu_0,+\mu_i^a)S_{Vb} \\ P_{33c}^m(\tau,-\mu_0,+\mu_i^a)S_{Ub} + P_{34c}^m(\tau,-\mu_0,+\mu_i^a)S_{Vb} \\ P_{43c}^m(\tau,-\mu_0,+\mu_i^a)S_{Ub} + P_{44c}^m(\tau,-\mu_0,+\mu_i^a)S_{Vb} \end{pmatrix}_{8N_1\times 1}.$$

From this expression it follows that if the incident beam source has no U and V components, then the sine modes of the $(I_\parallel, I_\perp)$ and the cosine modes of the (U,V) Stokes vector components vanish, in which case Eq. (72) provides the complete homogeneous solution as $\tilde{\mathbf{I}}_s^m = \mathbf{0}$.

Beam source

Consider now solutions for each of the source terms in Eq. (116). Thus, in a layer denoted by subscript ℓ, for the term $\tilde{\mathbf{X}}_{\alpha\ell}^m\, e^{-\tau/\mu_0}$, where $\tilde{\mathbf{X}}_{\alpha\ell}^m$ is assumed to be constant within layer ℓ, consider a particular solution of the form

$$\tilde{\mathbf{I}}_{\alpha\ell}^m(\tau) = \mathbf{Z}_{\alpha\ell}^m\, e^{-\tau/\mu_0}. \tag{121}$$

Substitution in Eq. (82) with $\tilde{\mathbf{Q}}_\alpha^m = \tilde{\mathbf{X}}_{\alpha\ell}^m\, e^{-\tau/\mu_0}$ leads to the following system of linear algebraic equations [$\mathbf{1}$ is the $8N \times 8N$ identity matrix]

$$[\tilde{\mathbf{A}}_\alpha^m + (\frac{1}{\mu_0})\mathbf{1}]\mathbf{Z}_{\alpha\ell}^m = \tilde{\mathbf{X}}_{\alpha\ell}^m \tag{122}$$

which can be solved to yield a particular solution vector $\mathbf{Z}_{\alpha\ell}^m$.

Thermal source

From the thermal source term, there is a contribution only for cosine mode $m = 0$ in the Fourier expansion; there is no contribution for any of the sine modes. To get an approximate particular solution to the inhomogeneous radiative transfer equation, one may make polynomial approximations to the Planck function and the source vector $\mathbf{S}_t(\tau)$:

$$B(T(\tau)) = \sum_{k=0}^{K} b_k \tau^k$$

$$\tilde{\mathbf{Q}}_t = \mathbf{U}^{-1}(1-\varpi(\tau))\sum_{k=0}^{K}\mathbf{D}_k\tau^k$$

where

$$\mathbf{D}_k \equiv \begin{pmatrix} \mathbf{D}_{1k} \\ \mathbf{D}_{0k} \\ \mathbf{D}_{1k} \\ \mathbf{D}_{0k} \end{pmatrix}_{8N\times 1} \qquad \mathbf{D}_{1k} \equiv \begin{pmatrix} b_k \\ \vdots \\ b_k \end{pmatrix}_{2N\times 1} \qquad \mathbf{D}_{0k} \equiv \begin{pmatrix} 0 \\ \vdots \\ 0 \end{pmatrix}_{2N\times 1} \tag{123}$$

where it has been taken into account that the thermal source is unpolarized. Since the thermal source term is non-vanishing only for the cosine mode $m = 0$, $\tilde{\mathbf{Q}}_c^m = \delta_{0m}\tilde{\mathbf{Q}}_t$, Eq. (82) becomes:

$$\frac{d\tilde{\mathbf{I}}_c^m(\tau)}{d\tau} = \tilde{\mathbf{A}}_c^m(\tau)\tilde{\mathbf{I}}_c^m(\tau) - \delta_{0m}\tilde{\mathbf{Q}}_t(\tau) \tag{124}$$

Thus, by substitution in Eq. (124) the assumption:

$$\tilde{\mathbf{I}}_c^m(\tau) = \delta_{0m}\sum_{k=0}^{K}\mathbf{X}_k^t\tau^k. \tag{125}$$

one obtains

$$\begin{aligned}\delta_{0m}\sum_{k=1}^{K}k\,\mathbf{X}_k^t\tau^{k-1} &= \delta_{0m}\tilde{\mathbf{A}}_c^m\sum_{k=0}^{K}\mathbf{X}_k^t\tau^k - \delta_{0m}(1-\varpi(\tau))\sum_{k=0}^{K}\mathbf{D}_k\tau^k \\ &= \delta_{0m}\Big[\tilde{\mathbf{A}}_c^m\sum_{k=1}^{K+1}\mathbf{X}_{k-1}^t\tau^{k-1} - (1-\varpi(\tau))\sum_{k=1}^{K+1}\mathbf{D}_{k-1}\tau^{k-1}\Big].\end{aligned}$$

Comparison of terms having equal powers of τ leads to

$$\begin{aligned} k < K+1 \quad &: \quad k\,\mathbf{X}_k^t = \tilde{\mathbf{A}}_c^0\mathbf{X}_{k-1}^t - (1-\varpi(\tau))\mathbf{D}_{k-1} \\ k = K+1 \quad &: \quad 0 = (\tilde{\mathbf{A}}_c^0\mathbf{X}_K^t - (1-\varpi(\tau))\mathbf{D}_K. \end{aligned}$$

The first order approximation ($K = 1$) is usually sufficient and yields

$$\tilde{\mathbf{A}}_c^0\mathbf{X}_1^t = (1-\varpi(\tau))\mathbf{D}_1 \tag{126}$$

and then we find $\mathbf{X}_0^t$ from

$$\tilde{\mathbf{A}}_c^0\mathbf{X}_0^t = (1-\varpi(\tau))\mathbf{D}_0 + \mathbf{X}_1^t. \tag{127}$$

6.4.4. General solution

For each Fourier component denoted by the superscript m, the general solution is a combination of the homogeneous solutions and the particular solutions for beam and thermal sources. Thus, the general solution is

$$\begin{aligned}\tilde{\mathbf{I}}_{\alpha\ell}^m(\tau) \;=\; &\sum_{j=1}^{8N}\tilde{C}_{\alpha j\ell}^m\tilde{\mathbf{G}}_{\alpha j\ell}^m e^{-k_{\alpha j\ell}^m\tau} + \mathbf{Z}_{\alpha\ell}^m e^{-\tau/\mu_0} \\ &+ \delta_{0m}\delta_{\alpha c}[\mathbf{X}_{0,\ell}^t + \mathbf{X}_{1,\ell}^t\tau], \qquad \ell = 1,\ldots,L. \end{aligned}\tag{128}$$

Since each of the solution vectors in the upper slab are of dimension $8N$, for example $\tilde{\mathbf{G}}^m_{\alpha j\ell} = [\tilde{G}^m_{\alpha j\ell}(1), \tilde{G}^m_{\alpha j\ell}(2), \ldots, \tilde{G}^m_{\alpha j\ell}(8N)]^T \equiv g^m_{\alpha j\ell}(i), i = 1, \ldots, 8N$, where the lower case letter g has been used to denote the vector component, one may rewrite Eq. (128) in component form as follows ($i = 1, \ldots, 8N$)

$$\begin{aligned} \tilde{i}^m_{\alpha\ell}(\tau, i) &= \sum_{j=1}^{8N} \tilde{C}^m_{\alpha j\ell} g^m_{\alpha j\ell}(i) e^{-k^m_{\alpha j\ell}\tau} + z^m_{\alpha\ell}(i) e^{-\tau/\mu_0} \\ &+ \delta_{0m}\delta_{\alpha c}[x^t_{0,\ell}(i) + x^t_{1,\ell}(i)\tau], \quad \ell = 1, \ldots, L. \end{aligned} \tag{129}$$

6.4.5. Boundary conditions

To complete the solution one must apply boundary conditions in order to determine the unknown coefficients, the $\tilde{C}^m_{\alpha j\ell}$'s, in Eq. (128). Mathematically, one is faced with a two-point boundary value problem, which requires a specification of the radiation field incident at the top and the bottom of the slab. In addition, at layer interfaces within the slab, the radiation field is required to be continuous because the refractive index is assumed to be constant within the slab. So, in summary, the following conditions are required

1. At the top of the slab the incident Stokes vector must be specified;
2. The Stokes vector must be continuous across layer interfaces within the slab, $\tilde{\mathbf{I}}^m_{\alpha\ell+1}(\tau_\ell) = \tilde{\mathbf{I}}^m_{\alpha\ell}(\tau_\ell)$;
3. At the bottom boundary the Stokes vector must be specified in terms of the bidirectional polarized (reflectance) distribution function.

Implementation of these conditions leads to a system of linear equations, and its solution yields the desired coefficients, the $\tilde{C}^m_{\alpha j\ell}$'s. For each layer there are $8N$ equations corresponding to the Stokes vector components at the $8N$ quadrature points. For L layers one obtains $8N \times L$ equations. Hence, one obtains a linear system of equations of dimension $(8N \times L) \times (8N \times L)$, and the solution of this linear system of equations will determine the $(8N \times L)$ unknown coefficients, the $\tilde{C}^m_{\alpha j\ell}$'s, required to complete the solution.

DISTRIBUTION LIST

DTIC/OCP
8725 John J. Kingman Rd, Suite 0944 Ft
Belvoir, VA 22060-6218 1 cy

AFRL/RVIL
Kirtland AFB, NM 87117-5776 2 cys

Official Record Copy
AFRL/RVBYI/Jeannette van den Bosch 1 cy

This page is intentionally left blank.